Power-to-Gas in gas and electricity distribution systems: A comparison of different modeling approaches

Power-to-Gas in gas and electricity distribution systems: a comparison of different modeling approaches

Gabriele Fambri[a], Cesar Diaz-Londono[a], Andrea Mazza[a], Marco Badami[a], Robert Weiss[b]

[a] *Dipartimento Energia, Politecnico di Torino, Corso Duca degli Abruzzi 24, 10129 Torino, Italy*

[b] *VTT Technical Research Centre of Finland Ltd., P.O. Box 1000, 02044 VTT, Espoo, Finland*

ABSTRACT

Power-to-Gas (P2G) has been one of the most frequently discussed technologies in the last few years. Thanks to its high flexibility, it can offer services to power systems, thereby fostering Variable Renewable Energy Sources (VRES) and the electricity demand match, mitigating the issues related to VRES overproduction. The analysis of P2G systems used at the distribution level has only been dealt with in a few studies: however, at this level, critical operation conditions can easily arise, in both the electrical infrastructure and in the gas infrastructure. The choice of appropriate modeling approaches for a P2G plant, as well as for the electricity and gas distribution grids is necessary to avoid overestimating or underestimating the potential flexibility that P2G plants connected to distribution networks can offer. The study presents a methodological analysis on the impact of different simulation approaches when P2G is installed at a distribution system level. The aim of this paper has been to understand the impact of different modeling approaches in order to determine whether, and under what conditions, they could be adopted. An illustrative case study has been developed to perform this analysis. The results show that the flexibility of the P2G technology can also be used at the distribution level; nevertheless, a correct modeling approach is necessary to properly evaluate the potential of this solution. The placement of P2G systems within the electricity network can affect the performance of the plant to a great extent. Therefore, it is necessary to use a model that takes into account the topology and energy flows of the electrical network. It was found, in the analyzed case study, that the use of an inappropriate electricity network model can lead, depending on the conditions, to either an overestimation or an underestimation (of 50% and 40%, respectively) of the ability of P2G plants to absorb VRES over-generation. The accuracy of the gas network and of the P2G plant models also plays an important role. In conditions of low gas consumption, it is necessary to consider the gas flows and the line-pack potential of the gas network, as well as the interactions between the components of the P2G plant in order to avoid underestimating the flexibility of the entire system. In the analyzed case study, the use of a simplified model of the gas network led to an underestimation of the accumulation potential of the over-generations of VRES of about 30%, while the use of a simplified model for the simulation of P2G plants led to a 10% underestimation of the storage potential.

KEYWORDS

Renewable energy integration, Electricity distribution system, Gas distribution system, Multi-energy system, Power-to-Gas, Modeling Approaches

ACRONYMS

BFS	Backward Forward Sweep
CH_4	Methane
CO_2	Carbon dioxide
DSO	Distribution System Operator
H_2	Hydrogen
HP	High Pressure
HV	High Voltage
G2P	Gas-to-Power
LHV	Lower Heating Value
LPEN	Lumped Parameter Electricity Network
LPGN	Lumped Parameter Gas Network
LPP2G	Lumped Parameter P2G
MP	Medium Pressure
MV	Medium Voltage
OLTC	On-Load Tap Changer
P2G	Power-to-Gas
$P2H_2$	Power-to-Hydrogen
P2X	Power-to-X

PEM	Polymer Electrolyte Membrane electrolyzer
PV	Photovoltaic plants
RPF	Reverse Power Flow
SNG	Synthetic Natural Gas
SoC	State of Charge
TR	Transformer
TSO	Transmission System Operator
VRES	Variable Renewable Energy Sources
WT	Wind Turbines

1. Introduction

1.1. Background

The average temperature throughout the world is about 0.8 °C higher than that of the pre-industrial level as a result of anthropogenic CO_2 emissions [1]. The European Union has defined the *Clean Energy for all Europeans* legislation package [2] with the intention of countering this dangerous trend, and renewable energies will play a fundamental role in this decarbonization process [3]. In order to preserve the correct and safe operation of an entire electricity network system, the energy generation and loads need to be instantaneously balanced and regulated. This delicate equilibrium may be undermined by Variable Renewable Energy Sources (VRES), which, due to their intrinsic high volatility, intermittency and low predictability nature, make it harder to achieve an electricity network balance [4]. New flexibility resources are needed to safely increase the renewable production and, at the same time, preserve the correct operation of an electricity system [5],[6]. Storage technologies, such as electric batteries [7], pumped hydro storage [8] and compressed-air energy storage [9], can offer a certain degree of flexibility, and allow the energy produced from renewable sources to be stored and dispatched in a flexible manner. Nevertheless, as also concluded in [10], in order to further increase the flexibility of an electricity system, it is necessary to review the paradigm of energy systems: in particular, if the entire system were considered, and not just the electricity sector, the global flexibility could increase significantly, thanks to the exploitation of new synergies between different energy-intensive sectors [11],[12]. Various sources of flexibility that fall outside the pure electricity sector have been analyzed in the literature, such as: thermal regulation systems for buildings [13],[14], electric mobility [15],[16], heat pumps connected to a district heating system [17] and district cooling networks [18]. The introduction of novel conversion technologies has made it possible to connect different energy sectors together. One of the most frequently discussed of these technologies is the Power-to-Gas (P2G) technology, which converts electrical energy into gaseous fuels.

1.2. Literature review

1.2.1. Overview of the P2G technology

The term P2G is used indiscriminately for both plants that produce pure hydrogen (through electrolyzers, supplied with electricity, which provide hydrogen through distilled water splitting) and for plants whose output is Synthetic Natural Gas (SNG). In the latter case, hydrogen, obtained from the electrolysis process, reacts with CO_2 to obtain methane (CH_4). This article only deals with the production of SNG: for this reason, from now on the term P2G will be used to indicate this type of technology, while the plants in which only hydrogen is produced will be indicated with the acronym $P2H_2$.
The main advantages of using P2G and $P2H_2$ technologies can be summarized in the following three points:

- they can be used to offer flexibility to a power system: in fact, thanks to the fast response of the electrolyzer, especially Polymer Electrolyte Membrane (PEM) electrolyzers, such a system can modulate its consumption over a wide range of operation points and quickly change them in a flexible way;
- they produce synthetic fuels: these fuels, if produced from renewable sources, can be used to decarbonize some final use sectors, whose electrification is less straightforward;
- They can be used as part of an energy storage system: in fact, they allow the electricity produced from renewable sources to be stored as chemical energy, which in turn can be converted into electricity, when needed.

Thanks to these features, P2G and $P2H_2$ technologies have been analyzed in the literature in different contexts. In [19], the P2G technology was analyzed to establish the absorption of the over-generations of wind energy and, at the same time, the possibility of participating in the frequency regulation of the electricity system. In [20], an energy hub with P2G was set up in a dynamic framework by considering the evolution of the energy demand, prices and the degradation of the components. The authors of [21] analyzed a P2G system coupled with other energy conversion technologies: P2G allowed the CO_2 emitted by gas boilers and combined heat and power plants to be significantly reduced. The use of the $P2H_2$ technology to refuel hydrogen vehicles in an microgrid context was analyzed in [22] and [23].. The use of the P2G technology to provide green fuel for heavy-duty vehicles in order to couple the electric and transportation sectors was discussed in [24]. The possibility of accumulating energy during a high production period from renewables in the form of synthetic fuels, and the conversion of these synthetic fuels into electricity, when necessary, was analyzed at a country level in [25] and at a microgrid level in [26].

1.2.2. Impact of P2G on electricity and gas distribution networks

When these energy conversion technologies are installed, it is necessary to analyze the impact they can have on the energy system into which they are introduced. In fact, these technologies allow the electricity sector and the gas sector to be connected. It is therefore necessary to analyze the effect of these connections in order, on the one hand, to optimize the use of these energy conversion plants and the energy flows in the grid infrastructures and, on the other hand, to prevent such plants from having a negative impact on the functioning of the overall multi-energy system.

It should be mentioned that P2G plants connected to transmission systems have been widely analyzed. The potential of P2G was evaluated in [27] for a regional scenario in Germany: the size of the considered P2G plants was optimized in order to minimize the levelized cost of electricity. The participation of an industrial P2G plant on the energy market and on the ancillary services market was analyzed in [28] and [29]. The role of P2G plants in a 2050 near zero carbon dioxide emission scenario was analyzed in [30]. In [31], the P2G technology was used to store VRES over-generation in a gas transmission system. It was concluded, in [32], that, thanks to the use of distributed resources, including P2G, it was possible to reduce renewable energy curtailment and, at the same time, increase social welfare. A 100% large, renewable, energy-based (wind and solar) city scenario was achieved in [33] by connecting electricity, gas and district heating networks through P2G plants.

However, as was concluded in [34], [35] and [36], the impact of P2G on a multi-energy system, when connected to a local distribution system, has so far only been analyzed in a few papers. Nevertheless, distributed flexible resources are gaining more and more importance for the control and regulation of power systems: as proof of this trend, the European Union is now working on fostering the participation of aggregate distributed sources on the market for ancillary services by offering flexibility to Transmission System Operators (TSO) [37]. In the future, as concluded in the SmartNet project [38], this kind of flexibility service could also be used by Distribution System Operators (DSOs) to balance their distribution networks. The presence of multi-energy infrastructures (such as gas and electricity networks) in the same district may be useful to help handle VRES over-generation at a distribution level, by reducing the effects witnessed for the transmission system, and actively supporting the regulation of the overall electricity system. Several small-scale P2G plants (300-700 kW of electrolyser) were used in [39] to absorb the surplus generation of PV in electricity distribution networks in a German region. In [40], the authors studied network voltage regulation using alkaline electroliers and an On-Load Tap Changer (OLTC); the same $P2H_2$ model was also used in [41] to optimize the size and allocation of plants connected to a distribution electricity network, with the goal of tackling the increasing penetration of VRES. A techno-economic analysis on the utilization of the $P2H_2$ technology was also analyzed in [35]: an energy conversion system was used to absorb the over-generation caused by the installation of PV plants on the distribution network. In this case, the use of an energy $P2H_2$ was evaluated and compared with an alternative network expansion solution. The coupling of electricity and gas distribution networks through the $P2H_2$ technology was analyzed in [42] and [43]; these articles analyzed how this technology affects the quality of the gas in the distribution network. The impact of the $P2H_2$ technology at the microgrid level was analyzed, from an economic point of view, in [26] and [23]. A real-time platform was presented in [44] to simulate distribution networks connected to P2G plants, and the paper also presented an analysis of a case study in which P2G systems operated as distributed resources to absorb the network Reverse Power Flow (RPF). The interaction between gas, electricity and district heating networks, enabled by P2G, was exploited in [45] in an attempt to reach the complete decarbonization of an energy system based on wind and solar energy. In [46], the authors defined the optimum size of a plant to optimize the system from a technical and economic point of view. In [36] and [47], the authors analyzed the possibility of providing voltage regulation in an electricity distribution system using P2G and the Gas-to-Power (G2P) technology. A novel P2G model, based on real data, was presented in [34], and this model, which was connected to an electricity distribution network with a high share of VRES distributed generation, was analyzed.

1.3. Scientific contribution

This paper presents an analysis of an electricity and gas multi-energy system scenario, developed as a follow-up to [48]. In that paper, the interactions between the electricity distribution grid, P2G plants and the gas network were analyzed through the use of *complete models* that were able to fully describe the possible interactions among all the elements. However, the aforementioned approach *i*) requires several data (which the owners may not be willing to disclose) and *ii*) can imply a high computation time, especially in the presence of annual scenarios. Hence, investigating *how* the calculation model can be simplified and *when* this simplification is effective, becomes necessary. These aspects have important implications, because, for example, they can impact the results of any control/optimization algorithm that uses the model to describe the physical behavior of the system.

On the basis of these premises, the aim of this paper is to present a complete analysis of the pros and cons of different modeling approaches and to describe the operation of the main elements of the multi-energy system, with particular focus on the *distribution* level. Such an analysis allows the issues of the most frequently used modeling approach, in which only one of the components that characterizes the multi-energy system is usually modeled in detail, to be overcome, while simplified models may be used for the other components.

Table 1 shows, as an example, that none of the aforementioned studies that focused on P2G in distribution systems analyzed the dynamics that take place between all three main components of a multi-energy system, i.e., the gas network, electricity network and P2G plants. Hence, this study aims to understand the effects of the *most common model simplifications* and to highlight whether, and in what cases, these simplifications could be acceptable. The modeling aspects analyzed in this paper are summarized as follows:

- The impact of including, or neglecting, the electricity distribution network topology on the results. This aspect is closely correlated with the aim of the study. The determination of the potential flexible resources that can be installed over a

wide area (in terms of power and energy capacity) is not affected to a great extent when a simplified version of High Voltage (HV) is considered (such as in [27], where the model only considers the equivalent capacity for different sub-regions, and in [49], where the potential of some flexible technologies was studied at a metropolitan level). However, if the aim of the study is to establish the impact of the distributed resources on the distribution system and the most effective location for the flexibility resources, the network topology has to be included, otherwise such aspects as the impact on *local over-generation* and network operation indicators (for example, the losses and voltage level) cannot be fully understood.

- The impact of gas network pressure dynamics. It is worth noting that the gas demand, when a high-pressure gas network is considered, is normally high enough to be able to absorb the SNG generated by the surplus of renewables [31], [50], and the effect of the "tank" (i.e., the gas grid) is therefore transparent with respect to the operation of the P2G plant. Accordingly, several studies have been carried out without considering any constraint related to the injection of gas into the gas network [27], [34], [49]. However, if the P2G plant is connected to a medium pressure (MP) distribution grid, the demand for natural gas might be very low, especially in the summer season, and may thus create a hurdle for SNG injection. Hence, using a complete gas network model, which considers the gas flow and the pressure in the pipes, allows the *line-pack* effect to be considered, and the pipeline volume could be used as a vessel to store natural gas inside the network itself. This intrinsic flexibility allows a temporal mismatch between the injected and withdrawn gas to be considered, which, if neglected, could lead to an underestimation of the SNG production of P2G plants, especially in the case of a low gas demand.
- The interaction between the internal units of a P2G plant, i.e., the electrolyzer, the hydrogen buffer and the methanation unit. In several papers (e.g., [32], [36], [47], [50], and [51]), the energy conversion process of a P2G plant was simplified by only taking into consideration the overall process efficiency, without considering the separate processes or the interactions between the internal components. This kind of approximation can lead to an underestimation of the flexibility of a P2G unit. In fact, if all the components are considered as single units, the electrolyzer, whose load should vary in order to offer flexibility to the electricity network, is limited by the operation of the methanation unit, which in turn is bounded by the constraints of the gas network. On the other hand, when the components are considered separately, the operation of the electrolyzer results to be more flexible, because the hydrogen is not absorbed directly by the methanation unit and is instead accumulated in the buffer.

In order to highlight the local flexibility potential enabled by the P2G technology, a suitable scenario was simulated through the use of models that take into account the physical phenomena listed above. Subsequently, the same scenario was simulated using simplified models to analyze whether, to what extent, and under what conditions these simplifications lead to an overestimation or underestimation of the performance of these plants. This methodology was set up to be an effective procedure to guide the reader in choosing the most appropriate modeling approach, by collecting all the conceptual and mathematical instruments necessary to effectively study multi-energy system with P2G at a distribution system level.

Table 1. Overview of previous studies on P2G in a distribution network scenario and the modeling assumptions.

Ref.	EN model		GN model		P2G model	
	Grid topology	Notes	Pressure dynamic	Notes	Sub-components	Notes
de Cerio Mendaza et al. 2015 [41]	**YES**	•Load flow analysis	NO	• A GN model was not included	NO	• Only P2H$_2$
Dalmau et al. 2015 [40]	**YES**	•Load flow analysis	NO	• A GN model was not included	NO	• Only P2H$_2$
Esterman et al. 2016 [39]	NO	•Load and generation balance	-	• No model details	-	• No model details were supplied
Khani et al. 2018 [47]	**YES**	•Load flow analysis	**YES**	• Gas flows calculated as a function of the nodal pressure	NO	• Entire process efficiency
Robinius et al. 2018 [35]	**YES**	•Load flow analysis (Gauss-Seidel method)	NO	• GN was not included	NO	• Only P2H$_2$
El-Taweel et al. 2019 [36]	**YES**	•Load flow analysis	**YES**	• Gas flows calculated as a function of the nodal pressure	NO	• Entire process efficiency
Salomone et al. 2019 [46]	NO	•Load and generation balance	NO	• A GN model was not included	**YES**	• Electrolyzer, H$_2$ storage and methanation unit models
Mazza et al. 2019 [42]	**YES**	•Load flow analysis (Backward Forward Sweep method)	**YES**	• Gas flows calculated as a function of the nodal pressure	NO	• Only P2H$_2$
Diaz-Londono et al.2020 [44]	**YES**	•Load flow analysis (Backward Forward Sweep method)	NO	• A GN model was not included	NO	• Entire process efficiency
Mazza et al. 2020 [34]	**YES**	•Load flow analysis (Backward Forward Sweep method)	NO	• A GN model was not included	**YES**	• Electrolyzer, H2 storage and methanation unit models
Weiss et al. 2021 [45]	NO	•Load and generation balance	NO	• A GN model was not included	**YES**	• Electrolyzer and methanation unit models
Cavana et al. 2021 [43]	**YES**	•Load flow analysis (Backward Forward Sweep method)	**YES**	• Gas flows calculated as a function of the nodal pressure	NO	• Only P2H$_2$
Shams et al 2021 [26]	-	•No model details	NO	• A GN model was not included	NO	• Only P2H$_2$
MansourLakouraj et al. 2021 [23]	-	•No model details	NO	• A GN model was not included	NO	• Only P2H$_2$
Fambri et al. 2022 [48]	**YES**	•Load flow analysis (Backward Forward Sweep method)	**YES**	• Gas flows calculated as a function of the nodal pressure	**YES**	• Electrolyzer, H$_2$ storage and methanation unit models
This paper	Comparison between the Backward-Forward-Sweep model approach and a load and generation balance approach		Comparison between an approach that takes into account the dynamics of network pressure and an approach that simplifies this aspect		Comparison between an approach that considers the subcomponents of P2G and an approach that only considers the efficiency of the P2G energy conversion efficiency	

1.4. The structure of the paper

The remainder of this paper is presented as follows: Section 2 introduces the multi-energy system scenario analyzed in this study; Section 3 reports the mathematical models of the multi-energy system components; the control logic of the P2G units is described in Section 4; Section 5 reports the results of the study, whereas Section 5 summarizes the conclusions.

2. The multi-energy system scenario

An illustrative multi-energy system scenario has been developed to carry out the aforementioned analyses (see Figure 1). The case study was presented in [48]. The multi-energy system includes a Medium Voltage (MV) electricity distribution network and an MP gas distribution network, coupled by means of P2G plants.

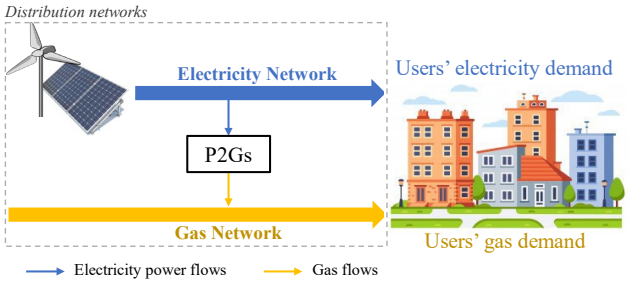

Figure 1. Multi-energy system scheme.

The data on the electricity and gas distribution network topologies were taken from real networks in northern Italy. The electricity distribution is related to an urban 22 kV-distribution system that operates in the City of Turin [52]: the network is composed of 43 electrical nodes, distributed over five feeders connected to the HV transmission system (220 kV) by means of three different HV/MV transformers (TRs) (see Figure 2a). The gas network topology was derived from [53]. The gas network is a medium-pressure network of the 4th species, according to the DM 24/11/1984 Italian classification [54] (operation pressure range: 1.5 – 5 bar_g). Considering the withdrawal nodes and the junction nodes, the network is composed of 70 nodes. The network has only one connection to the high-pressure (HP) transmission system, i.e., the city-gate at node 0. Gas can flow, through the city-gate, from the HP to the MP portions, but not in the other direction.

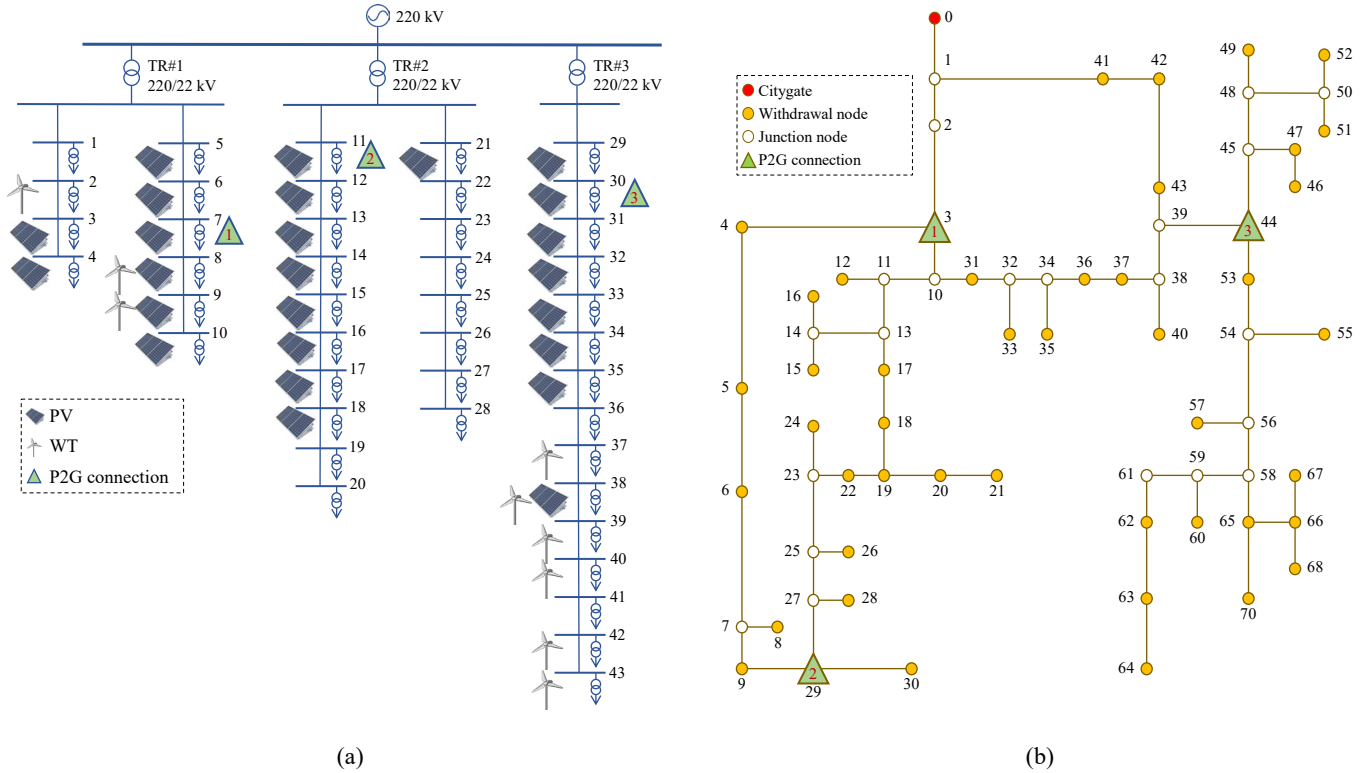

(a) (b)

Figure 2. Network topology and P2G connections. Electricity network (a). Gas network (b).

The scenario under analysis is characterized by a high number of installed VRES plants (photovoltaic plant, PV, and wind turbines, WT) connected to the electricity distribution grid. The scenario is assumed to cover electricity and gas users in the residential and

tertiary sectors. The gas demand is mainly for domestic purposes and to heat buildings. The installed power, the peak power, the total yearly energy of VRES generation, the electricity demand and the gas demand are summarized in Table 2, while the total monthly energy demand and generation are reported in Figure 3. It is possible to note that, during hot months (from April to September), the VRES production is nearly twice that of the rest of the year, due to the higher solar irradiation, while the electricity demand is almost constant throughout the whole year, with a slight increase in summer, due to the activation of building cooling systems. The gas consumption is the most seasonal dependent consumption: the gas demand during the coldest months is almost ten times higher than in summer, due to the high demand for building heating.

Table 2. Installed power, peak power and yearly energy of VRES, the electricity demand and the gas demand.

	Installed power [MW]	Peak power [MW]	Yearly energy [GWh]
PV	14.3	10.8	21.3
WT	4.4	3.9	3.4
El. demand	12.3	6.0	29.7
Gas demand	-	23.0	36.0

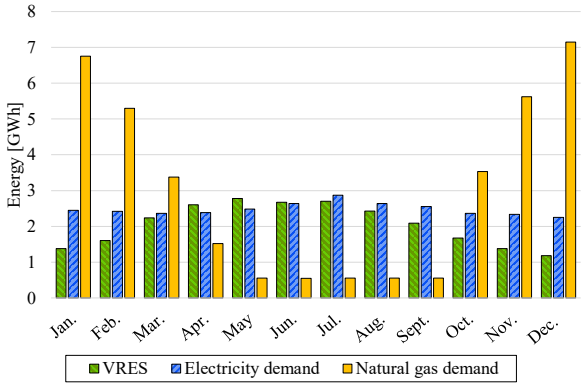

Figure 3. Monthly VRES generation, the electricity demand, and the gas demand.

These conditions generate two opposite situations in the hot and cold months. In fact, the winter months are characterized by a relatively low peak overproduction of renewable energy and a high demand for gas (see Figure 4c), while, in the summer months, during which the over-generation is higher, the demand for gas is considerably lower (see Figure 4b). The latter situation represents the most critical condition for the utilization of P2G flexible resources, because the large amount of VRES generation requires a higher exploitation of the P2G plants to balance the electricity network. However, the low gas demand could limit the injection of SNG into the gas network.

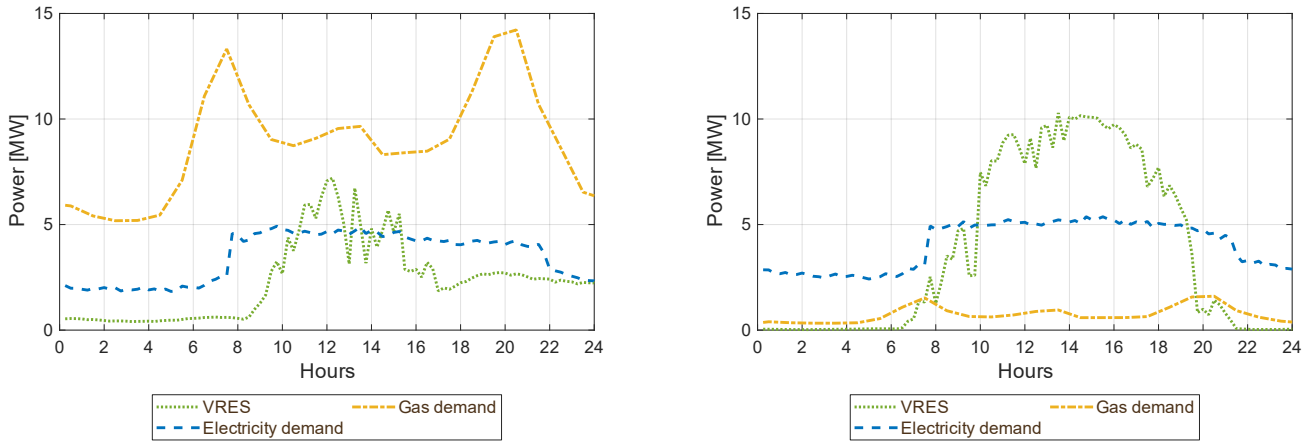

(a) (b)

Figure 4. VRES generation, the electricity demand, the gas demand for a winter day (a) and the gas demand for a summer day (b).

As shown in Figure 2, three P2G plants are connected to electricity nodes 7, 11 and 30 and to gas nodes 3, 29 and 44. The three P2G plants have the same technical characteristics (Table 3): each plant is composed of a 1200 kW Polymer Electrolyte Membrane (PEM) electrolyzer (referring to the electrical input power), a hydrogen buffer capable of storing up to 3060 kWh of hydrogen (about

92 kg, considering the Lower Heating Value, LHV, of hydrogen, which is equal to 33.3 kWh/kg) and a methanation unit with a maximum SNG output equal to 43.2 kg/h (about 600 kW, referring to the SNG_{LHV} output power).

Table 3. Size of the P2G plants and the network connections.

Parameter	Unit	P2G#1	P2G#2	P2G#3
Electrolyzer capacity	kW (el. input)	1200	1200	1200
Meth. unit capacity	kW (SNG output)	600	600	600
Hydrogen buffer capacity	kWh (H_2 LHV)	3060	3060	3060
El. network node connection	-	7	11	30
Gas network node connection	-	3	29	44

As depicted in Figure 2a, the electricity distribution network is connected to the high-voltage transmission network by means of three HV/MV transformers connected with a busbar. When the network generation is higher than the consumption, the electricity flows from the distribution to the transmission system, thus causing unbalances in the transmission system that need to be regulated by the TSO. It could also happen that VRES over-generation only occurs in one portion of the network: in this case, the over-generation flows through the transformer, the connection busbar and the other transformers, and is then absorbed by the remaining distribution system feeders. Even though this situation does not affect the transmission system, the flow can occur from MV to HV inside the transformer, i.e., RPF needs to be avoided by the DSO, as the network protection systems are not able to guarantee a proper operation of the distribution system under such circumstances [55], [56]. It is worth noting that solving the RPF of the distribution system will also indirectly solve the issues at the HV interface, because the variability of the local generation is not captured by the TSO. In order to highlight the impact of local unbalances, a critical scenario has been defined: as shown in Figure 5, almost 60% of the energy over-generation occurs in the network portion derived from TR#3.

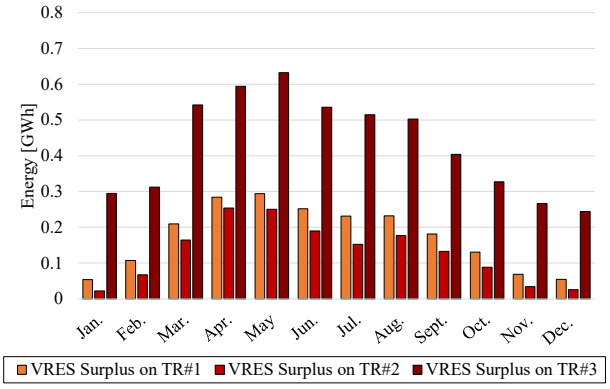

Figure 5. VRES over-generation (indicated in the figure as "Surplus") on the distribution network transformers.

3. The different modeling approaches

In order to evaluate the value of the modeling approaches, two models were considered for each component of the multi-energy scenario (electricity network, gas network and P2G): the first one takes into account the physics and internal dynamics of all the components, whereas the second one neglects them. These models were chosen to highlight three aspects of the multi-energy scenario: (*i*) the electricity network topology and the electricity flows in the network, (*ii*) the gas flows and pressure inside the gas network and (*iii*) the interactions between the sub-components of the P2G plant.

3.1. Electricity network modeling approaches

3.1.1. The complete electricity network model

The complete electricity network model takes into account the electricity flow in each branch, the voltage at each node and the withdrawals and injections of electricity at each node (see Figure 6). The analyzed electricity network is radial; under the hypothesis of the network being balanced (and this can be seen as a suitable approximation of the MV system), the power flow calculation, expressed as per unit, may be solved by applying the equivalent single-phase Backward-Forward-Sweep (BFS) algorithm [57]. The BFS considers N load nodes and B branches (with $N = B$, due to the radial network topology) and computes the current in the branches and the nodal voltages for each time step t as follows:

$$\begin{cases} \underline{\mathbf{i}}_{\mathrm{B},t}^{(k)} = \boldsymbol{\Gamma}^{\mathrm{T}} \cdot \underline{\mathbf{i}}_{\mathrm{N},t}^{(k)} = \boldsymbol{\Gamma}^{\mathrm{T}} \cdot \left[\underline{\mathbf{y}}_{\mathbf{C}} \circ \underline{\mathbf{v}}_t^{(k-1)} + \underline{\mathbf{s}}_t^{*} \oslash \left(\underline{\mathbf{v}}_t^{(k-1)} \right)^{*} \right] \\ \underline{\mathbf{v}}_t^{(k)} = \underline{\mathbf{v}}_{0,t} - \boldsymbol{\Gamma} \cdot \underline{\mathbf{Z}}_{\mathrm{B}} \cdot \underline{\mathbf{i}}_{\mathrm{B},t}^{(k)} \end{cases}, \forall\, t \in \mathbb{T} \quad (1)$$

where:

- $\underline{\mathbf{i}}_{\mathrm{B},t}^{(k)} \in \mathbb{C}^{B,1}$ represents the vector that contains the complex currents at time step *t*, calculated during the backward phase of the BFS method, at the *k*-th iteration;
- $\underline{\mathbf{v}}_{t}^{(k)} \in \mathbb{C}^{N,1}$ indicates the vector that contains the complex voltages at time step *t*, evaluated during the forward phase of the BFS method, at the *k*-th iteration;
- $\underline{\mathbf{i}}_{\mathrm{N},t}^{(k)} \in \mathbb{C}^{N,1}$ is the vector of the load nodes complex currents at time step *t*, at the *k*-th iteration;
- The inverse of the node-to-branch incidence matrix is the $\mathbf{\Gamma} \in \mathbb{N}^{B,N}$ matrix. This matrix provides topological information about the network;
- The load admittances and the network admittance are included in the $\underline{\mathbf{y}}_{\mathrm{C}} \in \mathbb{C}^{N,1}$ vector;
- $\underline{\mathbf{s}}_{t} \in \mathbb{C}^{N,1}$ is the net load vector of the constant power, which can be seen as the difference between the absorbed and injected power. A positive sign of the real (imaginary) part implies an absorption of active (reactive) power from the grid, whereas a negative sign indicates an injection of active (reactive) power into the grid. This representation is employed any time the power value at time step *t* is basically independent of the value of the node voltage at time step *t*;
- $\underline{\mathbf{v}}_{0,t} \in \mathbb{C}^{N,1}$ is the vector that contains the slack node voltage (indicated as 0 in Figure 6) at time step *t*;
- $\underline{\mathbf{Z}}_{\mathrm{B}} \in \mathbb{C}^{B,1}$ is a diagonal matrix that collects the values of the branch impedances;
- $\mathbb{T}$ is the set containing all the time steps.

Moreover, $\cdot$ is the inner product while the mathematical operators $\circ$ and $\oslash$ are the Hadamard product and division, respectively[1] [58], k refers to the calculation iteration, t to the time step and $\mathbb{T}$ is the set that contains all the horizon time steps. The symbol * indicates the conjugate operation. Finally, the symbols $\mathbb{N}$ and $\mathbb{C}$ represent the set of natural and complex numbers, respectively.
It is possible to calculate the RPF for each TR of the network at each time step t of the simulation. The RPF of the i-th TR at time step t, $RPF_{TR\#i,t}$, is calculated as:

$$E_{TR\#i,t} = real\left(\tau \cdot \underline{v}_{0,t} \cdot \underline{i}^{*}_{TR\#i,t}\right) \tag{2}$$

$$RPF_{TR\#i,t} = \begin{cases} -E_{TR\#i,t}, & if\, E_{TR\#i,t} < 0 \\ 0, & otherwise \end{cases} \tag{3}$$

where:

- $E_{TR\#i,t}$ is the energy flow through the TR#i at time step *t*;
- τ is time discretization (i.e., the duration referring to each time step, in our simulation 0.25 h);
- $\underline{v}_{0,t} \in \mathbb{C}$ is the voltage value of the electrical grid slack node at time step *t*;
- $\underline{i}_{TR\#i,t} \in \mathbb{C}$ is the currents of TR#i at time step *t*;

Further details on the EN model can be found in [52].

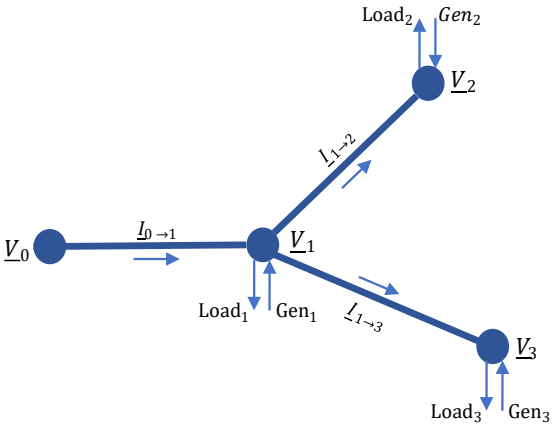

Figure 6. Scheme of the mathematical model of the electricity network.

3.1.2. The lumped parameter electricity network (LPEN) model
In the lumped parameter electricity network (LPEN) model, instead of simulating the whole electricity network, the electricity network is simplified by considering that all the loads and distributed generation are concentrated in a single node (see Figure 7).

[1] The Hadamard (or Schur) product and division are the element-by-element product and division, respectively. They are coded in Matlab® with the ".*" and "./"terms.

The RPF is calculated as the positive difference between the sum of the distributed generations in the network and the sum of all the loads. If the network distributed generation is lower than the network energy demand, the difference is assumed to be provided by the HV network:

$$RPF_t = \begin{cases} \sum_{n=1}^{N} gen_{n,t} - load_{n,t}\,, & if \sum_{n=1}^{N} gen_{n,t} - load_{n,t} > 0 \\ 0, & otherwise \end{cases} \quad (4)$$

$$HV_{\text{el},t} = \begin{cases} \sum_{n=1}^{N} load_{n,t} - gen_{n,t}\,, & if \sum_{n=1}^{N} load_{n,t} - gen_{n,t} > 0 \\ 0, & otherwise \end{cases} \quad (5)$$

where:

- RPF_t is the network RPF at time step t;
- $HV_{\text{el},t}$ is the electricity withdrawn from the HV network at time step t;
- $gen_{n,t}$ is the electricity generation at node n at time step t;
- $load_{n,t}$ is the electricity load at node n at time step t.

The three connections to the high voltage network (i.e., the three transformers) are not considered separately, but merged into a single connection point. The model is not able to identify any local VRES over-generation that can affect the distribution network transformers, but only the total VRES over-generation that affects the transmission system.

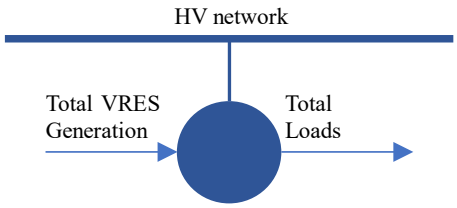

Figure 7. Scheme of the electricity network lumped parameter model.

3.2. Gas network modeling approaches

3.2.1. The complete model of the gas network

The complete model of the gas network takes into account the gas flow in each pipe and the pressure at each node of the network (see Figure 8). The model is based on the Renouard equation for a medium pressure pipeline [59] (Renouard's equation was inverted to isolate the gas flow between two nodes: Eq. 6), the equation of state for ideal gases (Eq. 7) and the continuity equation (Eq. 8). The mass flow between two nodes is determined from their pressure difference through the Renouard relation: the gas flow between node m and node n is positive, if the pressure at node m is higher than that of node n, and negative (flowing in the opposite direction) for the opposite situation, i.e., the model is bi-directional. The pressure of each node is calculated using the equation of state as a function of the pressure and mass that exist at the node. The gas mass at the node is given by the continuity equation, which considers the gas injections and withdrawals, as well as the gas flows that go from that node to the adjacent ones.

$$\dot{m}_{m-n,t}^{(\vartheta)} = \left| \frac{{p_{m,t}^{(\vartheta-1)}}^2 - {p_{n,t}^{(\vartheta-1)}}^2}{25.24 \cdot L_{m-n} \cdot {D_{m-n}}^{-4.82}} \right|^{\frac{1}{1.82}} \cdot \rho_{NG} \cdot sgn\left(p_{m,t}^{(\vartheta-1)} - p_{n,t}^{(\vartheta-1)}\right) \quad (6)$$

$$\frac{dp_{m,t}(\vartheta)}{d\vartheta} = \frac{p_{m,t}^{(\vartheta)} - p_{m,t}^{(\vartheta-1)}}{d\vartheta} = \frac{R_{NG} \cdot T}{V_m} \cdot \dot{m}_{m,t}^{(\vartheta)} \quad (7)$$

$$\dot{m}_{m,t}^{(\vartheta)} = \dot{m}_{inj,m,t} - \dot{m}_{wit,m,t} + \sum_{n=1}^{N_m} \dot{m}_{m-n,t}^{(\vartheta)} \quad (8)$$

where:

- $\dot{m}_{m-n,t}^{(\vartheta)}$ is the natural gas flow inside pipe $m-n$ at time step t and at the iteration of the integration procedure ϑ (the subscript n represents a generic node of the nodes adjacent to node m);
- $p_{m,t}^{(\vartheta-1)}$ and $p_{n,t}^{(\vartheta-1)}$ are the pressures of nodes m and n, respectively, at time step t and at the iteration of the integration procedure $\vartheta - 1$;

- L_{m-n} is the length of pipe $m-n$;
- D_{m-n} is the diameter of pipe $m-n$;
- ρ_{NG} is the natural gas density under standard conditions;
- $p_{m,t}^{(\vartheta)}$ is the pressures in nodes m at time step t and at the iteration of the integration procedure ϑ;
- $d\vartheta$ is the integration step;
- R_{NG} is the specific gas constant of natural gas;
- T is the temperature of natural gas;
- V_m is the volume of the node;
- $\dot{m}_{m,t}^{(\vartheta)}$ is the mass variation at node m at time step t and at the iteration of the integration procedure ϑ;
- $\dot{m}_{inj,m,t}$ and $\dot{m}_{wit,m,t}$ are the gas injection and withdrawal at node m, respectively, at time step t;
- N_m is the number of nodes adjacent to node m.

By combining equations (6), (7) and (8), it is possible to define the evolution of the pressure of each node of the network as a function of the gas inputs and withdrawals at the node and the pressures of the adjacent nodes:

$$P_{m,t}^{(\vartheta)} = P_{m,t}^{(\vartheta-1)} + d\vartheta \cdot \frac{R_{NG} \cdot T}{V_m} \cdot \left\{ \dot{m}_{inj,m,t} - \dot{m}_{wit,m,t} + \sum_{i=1}^{\mathrm{N}} \left[\left| \frac{{p_{m,t}^{(\vartheta-1)}}^2 - {p_{n,t}^{(\vartheta-1)}}^2}{25.24 \cdot L_{m-i} \cdot {D_{m-i}}^{-4.82}} \right|^{\frac{1}{1.82}} \cdot \rho_{NG} \cdot sgn\left(p_{m,t}^{(\vartheta-1)} - p_{n,t}^{(\vartheta-1)}\right) \right] \right\} \tag{9}$$

while the model assumes, as a boundary condition, that the pressure at the city-gate (node 0) is always equal to 4 bar. Gas can flow through the city-gate (node 0) from the high-pressure network to the medium-pressure network, but not vice versa. If the pressure at node 1 is lower than the city-gate pressure, natural gas flows from the city-gate (coming from the transmission network) to node 1. If the pressure at node 1 is higher than the city-gate pressure, the gas flow between node 1 and the city-gate is 0:

$$NG_{NG,t}^{(\vartheta)} = \dot{m}_{0-1,t}^{(\vartheta)} = \begin{cases} \left(\frac{{p_{0,t}^{(\vartheta-1)}}^2 - {p_{1,t}^{(\vartheta-1)}}^2}{25.24 \cdot L_{0-1} \cdot {D_{0-1}}^{-4.82}} \right)^{\frac{1}{1.82}} \cdot \rho_{NG}, & if\ p_{0,t}^{(\vartheta-1)} - p_{1,t}^{(\vartheta-1)} > 0 \\ 0, & otherwise \end{cases} \tag{10}$$

where $NG_{NG,t}^{(\vartheta)}$ is the natural gas withdrawn from the high-pressure transmission network at time step t and at the iteration of the integration procedure ϑ.

The model calculates the pressure in all the nodes of the network and the gas flows in each pipe of the network. This makes it possible to analyze how the volume of the gas network can be exploited to accumulate the gas inside the network, thanks to the line-pack effect: storing gas inside the pipes increases the internal pressure of the network, and the accumulation can continue until the network pressure reaches the network operating pressure limit (in this case, 5 bar_g). If this feature were not taken into account, the injection of SNG into the network would be constrained by the instantaneous demand for gas, while, thanks to the physics of this system, the gas network allows a more flexible use of the methanation units. The storage capacity of the gas network, SNG_{max_t}, is calculated at each simulation time step as:

$$SNG_{max_t} = \left(\sum_{m=1}^{\mathrm{M}} \dot{m}_{wit,m,t} \cdot \tau \right) + \frac{(p_{max} - \bar{p}_t) \cdot 10^5 \cdot V_{tot}}{R_{NG} \cdot T} \tag{11}$$

where:

- M is the number of nodes in the gas network;
- p_{max} is the operating pressure limit of the gas network;
- $\bar{p}_t$ represents the mean pressure of the gas network at time step t;
- V_{tot} represents the volume of the entire gas network.

More details on the GN model are reported in [48].

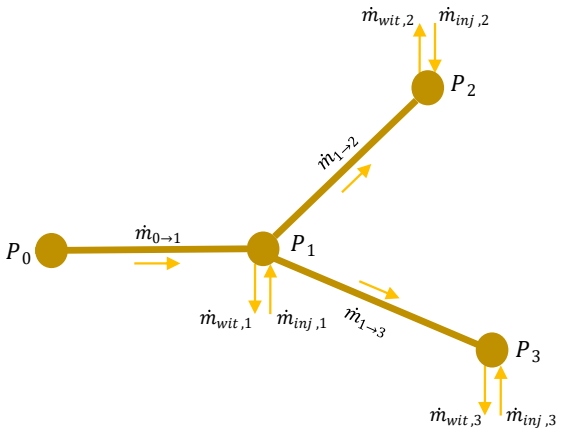

Figure 8. Scheme of the mathematical model of the gas network.

3.2.2. The lumped parameter gas network (LPGN) model

The lumped parameter gas network (LPGN) model does not take into account either the pressure evolution of the network nodes or the gas flow in each network pipe. All the users' gas withdrawals and SNG injections are considered to happen at the same points (see Figure 9). If the gas demand is higher than the SNG injection, the difference is taken from the HP network:

$$HP_{NG,t} = \begin{cases} \sum_{m=1}^{M} \left(\dot{m}_{wit,m,t} - \dot{m}_{inj,m,t}\right) \cdot \tau, & if \sum_{m=1}^{M} \dot{m}_{wit,m,t} - \dot{m}_{inj,m,t} > 0 \\ 0, & otherwise \end{cases} \quad (12)$$

where $HP_{NG,t}$ is the NG withdrawn from the high-pressure transmission network at time step t.

The model cannot take into account the line-pack effect: hence, SNG can be injected as long as it does not exceed the gas demand:

$$SNG_{max_t} = \sum_{m=1}^{M} \dot{m}_{wit,m,t} \quad (13)$$

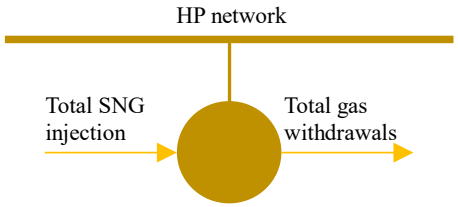

Figure 9. Scheme of the gas network lumped parameter model.

3.3. The P2G modeling approaches

3.3.1. The complete model of the P2G plant

The main components of the P2G plant are the PEM electrolyzer, the hydrogen buffer and the methanation reactor (see Figure 10). The hydrogen buffer allows a decoupling to be made between the electrolyzer and the methanation unit. The produced hydrogen is accumulated in the buffer, and, in this way, the electrolyzer can work, even though, at that moment, the methanation unit does not use the produced hydrogen. Similarly, the methanation unit can use the hydrogen previously produced by the electrolyzer and operate independently. The electrolyzers are controlled to absorb the renewable over-generations that affect the distribution network transformers. The PEM electrolyzers are able to change their setpoint very quickly, in less than 2 seconds; since the simulation is performed with a time discretization step of 15 minutes, the ramp limit for the electrolyzers has been neglected. The model is based on a non-linear experimental-based operating curve [60] which defines the hydrogen thermal output power as:

$$H_{2_{PEM,th,t}} = -\frac{0.24}{EL_{PEM,max}} \cdot {EL_{PEM,t}}^2 + EL_{PEM,t} - 0.055 EL_{PEM,max} \quad (14)$$

where:

- $H_{2_{PEM,th,t}}$ is the hydrogen output power (defined considering its highest heating value, that is, 12.75 MJ/Nm^3) at time step t;

- $EL_{PEM,max}$ is the electric nominal capacity of the PEM electrolyzer;
- $EL_{PEM,t}$ is the electric input of the PEM electrolyzer at time step t.

The produced hydrogen is accumulated inside the buffer: if the buffer reaches the maximum operating pressure (30 bar), the accumulation of hydrogen should be stopped. The minimum pressure of the storage is 7.2 bar. The pressure of the hydrogen buffer is calculated as a function of the mass of hydrogen accumulated in the buffer according to the equation of ideal gases. The state of charge of the storage is defined as a function of the storage pressure and the maximum and minimum pressure limits:

$$SoC_{ST,t} = \frac{p_{ST,t} - p_{ST,min}}{p_{ST,max} - p_{ST,min}} \cdot 100 \quad (15)$$

where:

- $SoC_{ST,t}$ is the state of charge of the hydrogen buffer at time step t;
- $p_{ST,t}$ is the pressure of the hydrogen buffer at time step t;
- $p_{ST,min}$ and $p_{ST,max}$ are the minimum and the maximum pressure of the hydrogen buffer respectively.

The methanation reactor model considered in this study simulates the operation of a catalytic methanation unit. The methanation reactor is maintained in hot stand-by, and when the hydrogen buffer reaches a pressure of 15 bar, the unit is turned on. The upward and downward ramp rate constraints of the methanation reactor limit the load variation of these units: the maximum upward ramp rate is 3.8 kg/h, while the maximum downward ramp rate is 46 kg/h. As a result of the technical limitations of this technology, the methanation unit cannot work below 50 % of its nominal capacity without being shut down. If the gas network reaches its maximum working pressure (5 bar_g), SNG generation should be limited to keep the gas network within the allowed pressure range.
The methanation unit model is a surrogate model that has been derived from the simulation data provided by a high-fidelity model [61] realized with the Apros® dynamic process simulator [62]. The surrogate model was fitted using a lasso regression analysis method performed using the Alamo (Automatic Learning of Algebraic MOdels) tool [63]. Using data from the Apros® dynamic model, Almo found a linear correlation between the hydrogen input power and the SNG power output (SNG_{th}):

$$SNG_{MET,th,t} = a_1 \cdot H_{2_{th,t}} - a_0 \quad (16)$$

where:

- $SNG_{MET,th,t}$ is the Synthetic Natural Gas output power at time step t;
- a_1 and a_0 are the coefficients of the surrogate model, which depend on the size of the methanation reactor.

Further details on the complete P2G model can be found in [64].

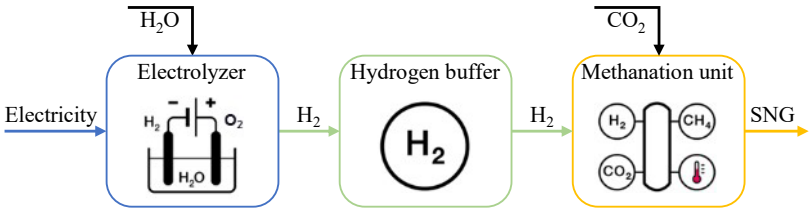

Figure 10. Scheme of the complete P2G model, adapted from [65].

3.3.2. The lumped parameter P2G (LPP2G) model
In this case, the P2G model does not consider the interaction between the main components of the plant. The entire process is summarized by means of fixed conversion efficiencies (see Figure 11). The electricity consumed by the plant is converted directly into SNG, without considering the internal dynamics of the plant, such as the hydrogen accumulation in the buffer, the methanation unit ramp rates or the minimum load constraints. The electricity consumption and SNG generation are thus temporally linked to each other:

$$SNG_{MET,th,t} = \eta_{P2G} \cdot \left(EL_{P2G,t} - EL_{aux}\right) \quad (17)$$

where:

- η_{P2G} is the efficiency of the entire energy conversion process;

- $EL_{P2G,t}$ is the electricity consumption of the plant at time step t;
- EL_{aux} is the electricity consumption of the auxiliary components, which is considered to be constant and equal to 1% of the nominal electrical load of the plant.

For the sake of consistency, η_{P2G} was set equal to the average efficiencies over the full year, as simulated by the complete model.

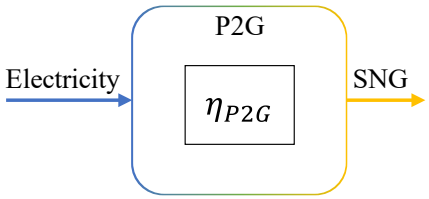

Figure 11. Scheme of the P2G lumped parameter model.

4. Simulation control algorithm

In this study, each P2G plant is connected to a feeder derived from a different HV/MV transformer (see Figure 2a), so that it can tackle all the local VRES over-generations that may exist within its feeders. Thanks to their fast response and high flexibility, PEM electrolyzers are in fact able to follow the fast variation of VRES [66],[67]. Under normal conditions, when there are no VRES over-generations, the electricity consumption of the P2G plants is kept at its minimum load, i.e., the electricity consumption needed to keep the systems under standby. When a local VRES over-generation occurs, the PEM electrolyzer of the plant connected to the part of the network that is affected by over-generation is turned on. When the scenario is simulated using the simplified EN model, since it is not possible to identify in which part of the electricity grid the overproduction occurs, the excess energy is distributed equally over the three P2G plants. The electrolyzer is used to absorb all the VRES over-generation as long as the following two constraints are respected: *i*) the electrolyzer cannot work at a greater power than its nominal capacity and, *ii*) the plant cannot exceed the production limits (see Figure 12). The production limits are determined by the hydrogen buffer: the plant can absorb electricity as long as the produced hydrogen can be accumulated in the buffer. If the buffer reaches the maximum state of charge, the PEM must limit its electricity absorption. When the scenario is simulated with the P2G lumped parameter model, the intermediate processes that occur within the P2G plant are not taken into account. The model considers that electricity is transformed directly into SNG. Thus, if the gas network cannot absorb SNG, the electrical consumption of the system is also limited.

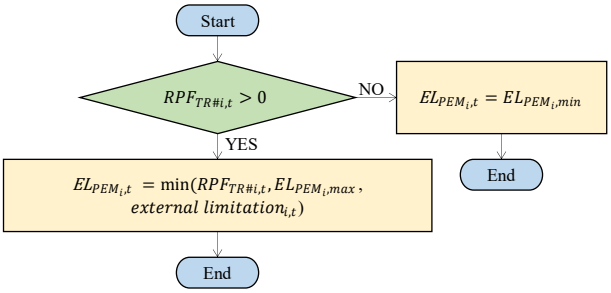

Figure 12. Algorithm for the control of the *i*-th electrolyzer at time step t.

In simulations carried out with the complete P2G model, the methanation unit is turned on when the hydrogen buffer reaches 50% of the state of charge. The methanation process continues until the buffer is completely empty. A limitation of injectable SNG in the network may occur in periods of low gas demand. In this case, some of the methanation units may have to limit the production of SNG or even stay in stand-by conditions until the network is once again able to absorb SNG. If the production of one or more plants has to be limited, the production priority is given to the plants that are already in the operational phase (e.g., if the methanation unit of plant X is already in the operational phase, it is not switched off to allow the plant Y methanation unit in standby to start producing). As a second priority criterion, priority is given to units whose hydrogen buffer has the highest state of charge. The units in a stand-by condition are activated only if the gas network is able to further absorb SNG and if the units in running condition are already working at the maximum load (see Figure 13). The maximum amount of SNG that can be injected into the gas network is defined at each step by the gas network model as a function of the gas demand and also, in the case when the complete gas network model is used, by the flexibility made available by the line-pack effect.

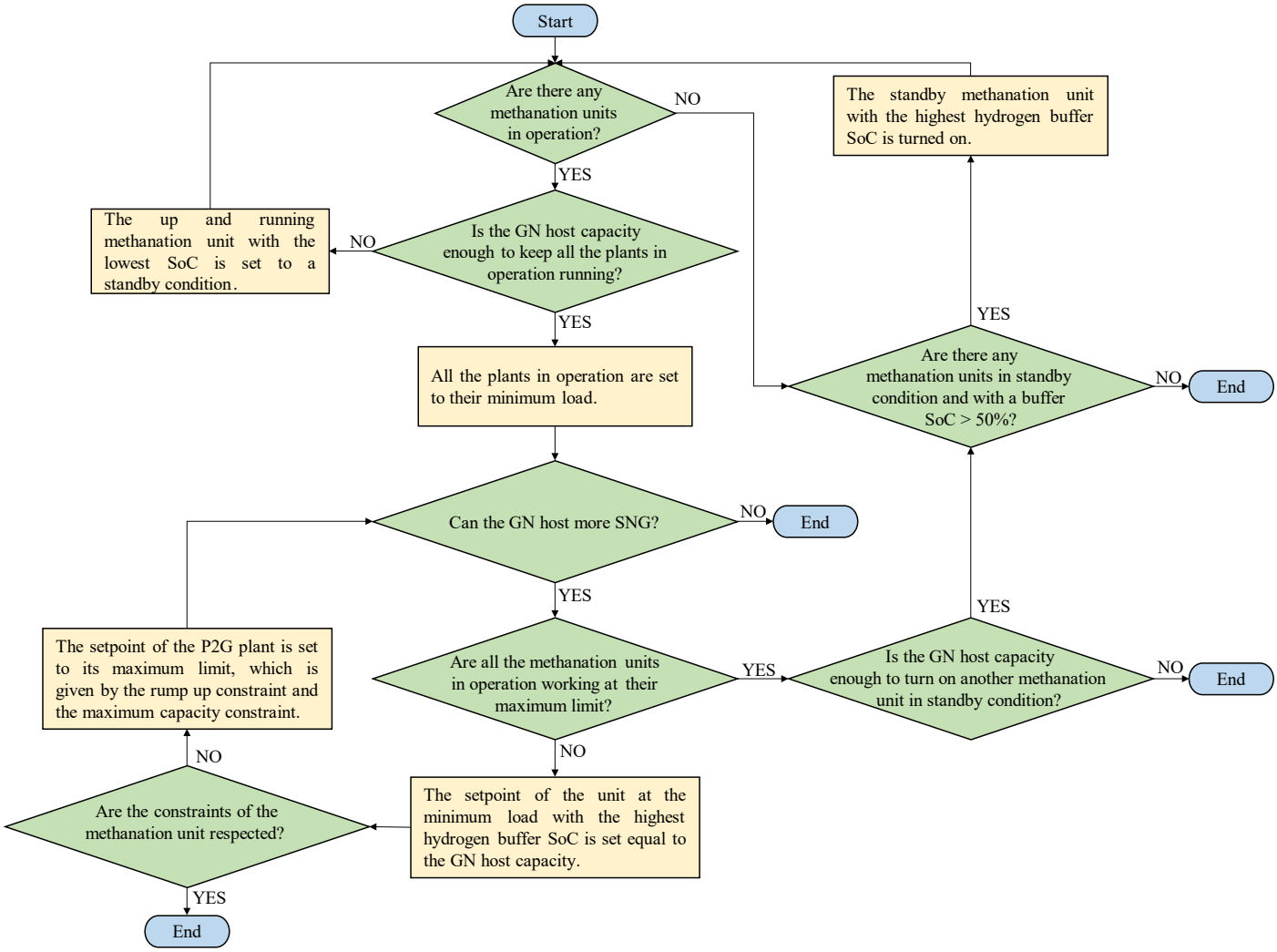

Figure 13. Algorithm for the control of the methanation units.

5. Results

This section shows the results of the simulations conducted with the various models. The first simulation (called Reference simulation) was carried out using the complete models of all three components of the multi-energy scenario. Subsequently, three other simulations were made, each time neglecting a different aspect of the modeling. The results of the various simulations were then compared with the Reference simulation. Table 4 summarizes the simulations that were carried out and the models that were used.

Table 4. List of simulations.

	EN model	GN model	P2G model
Reference simulation	Complete	Complete	Complete
LPEN simulation	***Simplified***	Complete	Complete
LPGN simulation	Complete	***Simplified***	Complete
LPP2G simulation	Complete	Complete	***Simplified***

5.1. P2G flexibility in the distribution systems

The electricity flowing in the three transformers of the electricity grid for a typical winter day are represented in Figure 14. It can be noted that the VRES production causes local over-generations, which in turn affect all the three transformers of the network, but with greater intensity in the part of the network downstream of the TR# 3. The flexibility offered by the P2G plants allows most of the over-generations of VRES to be absorbed. When the over-generation of VRES is higher than the nominal capacity of the P2G plants (1.2 MW_e), it cannot be fully absorbed and therefore causes an RPF in the transformers (see the orange area in Figure 14). During the heating season, the demand for gas is high enough to avoid causing a constraint on the operation of the methanation units: when the SNG is injected, it is immediately consumed by the users connected to the gas network (see Figure 15).

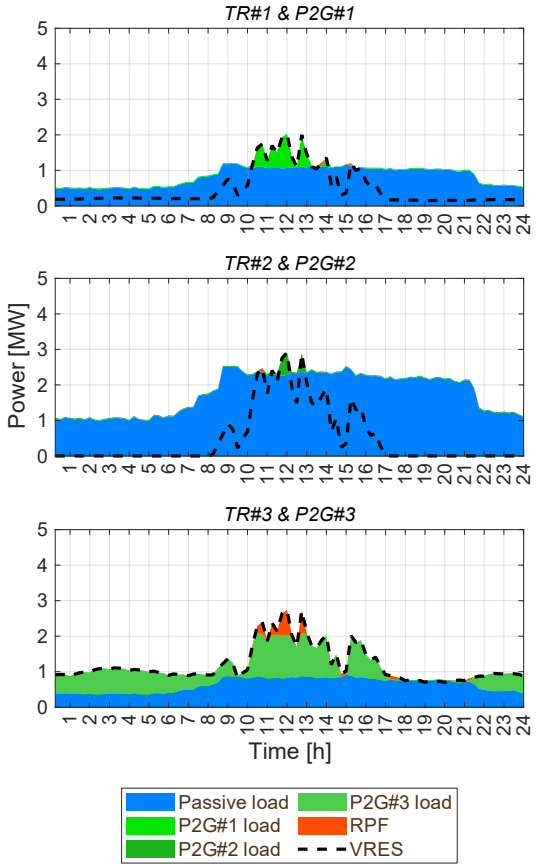

Figure 14. Electricity balance on HV/MV transformers (winter day) – Reference simulation.

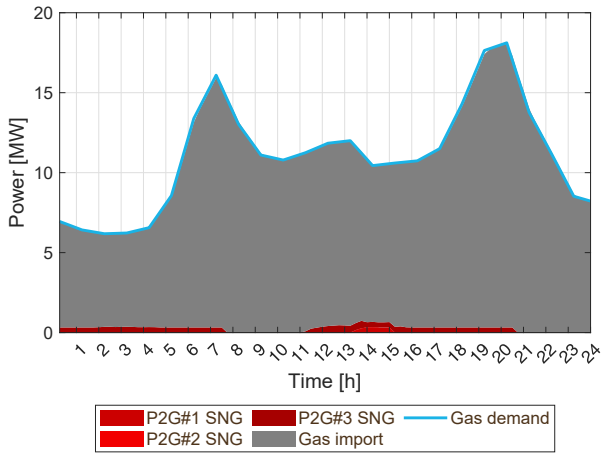

Figure 15. Gas network balance (winter day) – Reference simulation.

The VRES generation is higher in summer than in winter; hence, the RPF on the transformers increases (see the orange areas in Figure 16). The demand for gas is highly seasonal, due to the use of gas to heat buildings: the gas demand during the hot season is about 10 times lower than in the winter season. The SNG production in summer could exceed the users' gas demand (see Figure 17[2]); when this happens, the produced SNG could be stored by exploiting the gas network volume, thanks to the line-pack effect. The accumulation of gas increases the pressure in the network (see the dashed black curve in Figure 17). When the maximum operating pressure in the network is reached, the SNG injection should be reduced (in the case reported in Figure 17, the pressure reaches a level of 5 bar_g at 15:15 and the P2G#1 and P2G#2 methanation units block their SNG injection to allow the network to lie within its operation pressure range). The accumulated SNG is used in the following hours to meet the gas demand (see the white

[2] For clarity, the y-axis in the figures representing gas flows have different scales.

areas in Figure 17): when this happens, the gas stored inside the network decreases, as does the network pressure. It should be noted that, although at 15.15 the methanation units of P2G#1 and P2G#2 are in stand-by condition, these P2G plants can continue to absorb renewable over-generation and produce hydrogen. Even though it is not directly consumed by the methanation unit, the hydrogen can be accumulated inside the plant buffer. The electrolyzer can continue to absorb the over-generations and produce hydrogen until the buffer reaches the maximum state of charge (see the dotted lines in Figure 16).

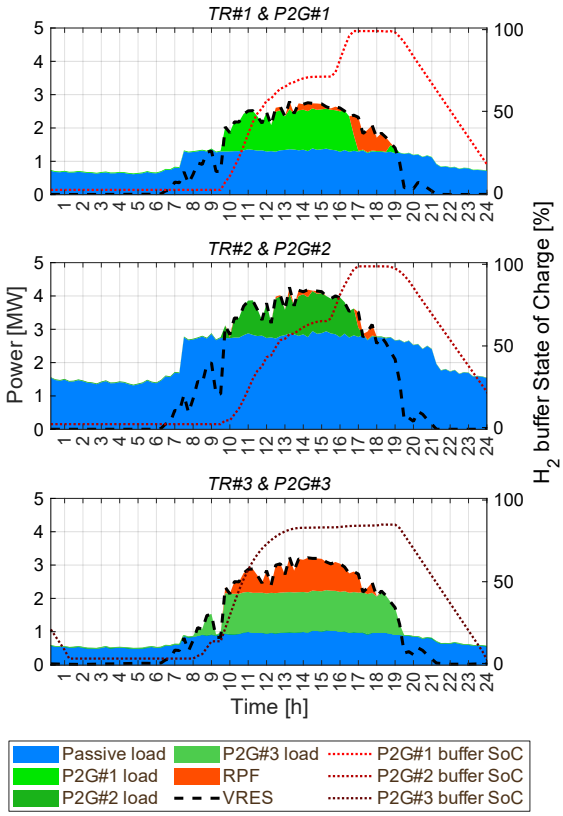

Figure 16. Electricity balance on HV/MV transformers and P2G hydrogen buffer SoC (summer day) – Reference simulation.

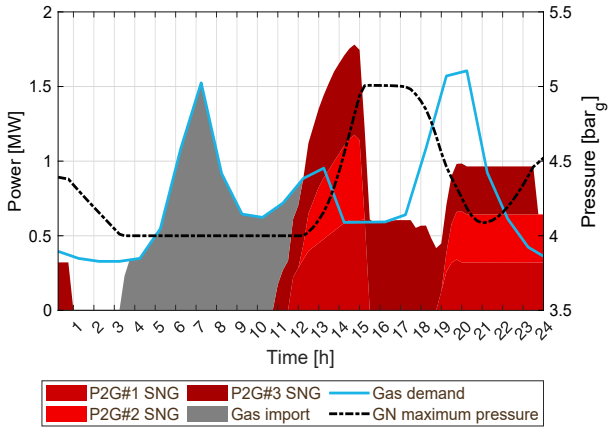

Figure 17. Gas network balance and pressure (summer day) – Reference simulation.

5.2. The value of electricity network modeling

The electricity network lumped parameter model does not consider the different HV/MV connection points. Even though the overall network is balanced, in terms of energy generation and consumption, the optimum operation condition may not have been reached due to a local load/generation mismatch. Figure 18 compares the energy balance of the whole electricity network in the Reference simulation versus the one simulated with the lumped parameter electricity network for a typical winter day. The LPEN model underestimates RPF: in fact, the P2G plants in LPEN appear to be able to absorb all the VRES over-generation, while the VRES over-generations in the Reference simulation are not totally absorbed, thus causing an RPF (see the orange area in Figure 18a).

Moreover, it seems that P2G#3 is activated in the Reference simulation, even when there is no need to actively absorb over-generation (i.e., during the nighttime). However, if the energy balance is computed at each HV/MV transformer level, local unbalances appear (see Figure 19)[3]. Since the lumped parameter model is not able to define where the over-generation occurs, the activation of the P2G plants has not been properly coordinated. It could happen that a P2G is sometimes activated, even though there is no need to absorb local unbalances (see the balance of TR#2 in Figure 19) and that some local VRES over-generations are not detected by the lumped parameter model (see the balance of TR#3 in Figure 19). For these reasons, the optimal coordination of various P2G plants cannot be achieved and P2G#3 results to be used about 40% less frequently than the Reference simulation, while P2G#2 is used about 50% more (see Table A. 1). It can be noted that, in the LPEN simulation, the P2G load (i.e., the sum of the electricity consumption of all three plants) is around 10% *lower* than in the Reference simulation, and this also affects the total SNG production of the plants, which leads to an underestimation of the injection of SNG into the gas network (see Table A. 3). This is due to the underestimation of the local RPF, whose sum results to be higher than the one that is seen by the transmission system. It is worth noting that the more diverse the local electricity imbalances are, the more marked the difference between the two models: in fact, the generation disparity within the network is greater in the winter months (in this period, about 65% of the over-generation takes place in the network portion derived from TR#3) and the difference in the use of P2G plants is about 20%. Unlike the winter months, the local grid mismatches are more homogeneous in the summer months, and the difference between the two modeling approaches is reduced to about 5%.
The VRES over-generation, calculated with Eq. 2 (without considering the losses due to the Joule effect), corresponds to the network unbalance that affects the transmission system. Thus, even though the simplified model does not allow an optimum dispatchment of the P2G plant utilization or the evaluation of the best P2G plant network connection, it could be used for a high-level qualitative evaluation of the P2G flexibility potential for transmission system balancing purposes (as shown in [46] and [49]).

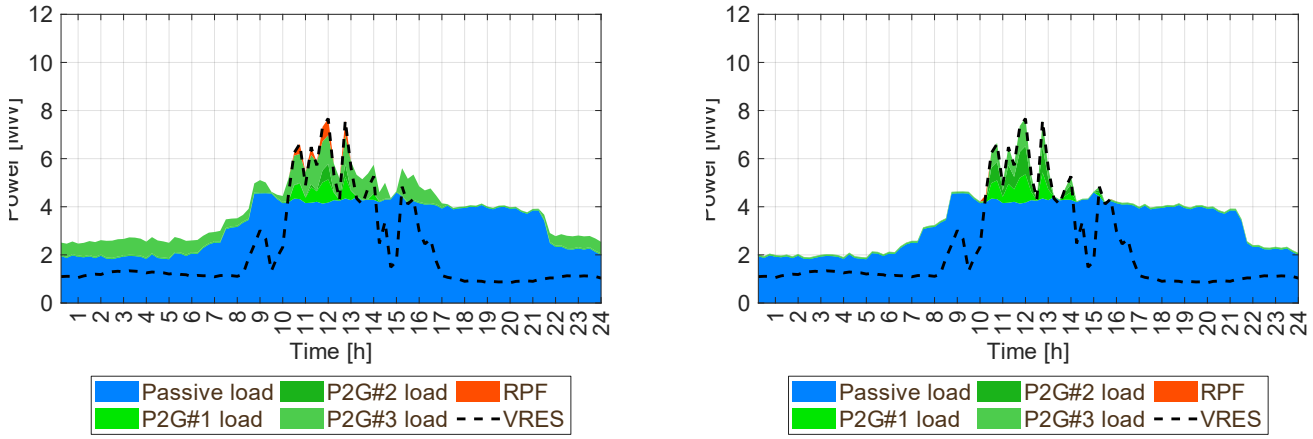

Figure 18. Electricity balance referring to the whole grid (winter day) – (a) Reference simulation and (b) LPEN simulation.

[3] In order to evaluate the local unbalances in the LPEN simulation (which does not consider the HV/MV transformers), the reference model of the electricity network was run with P2G electricity load profiles obtained from the LPEN simulation.

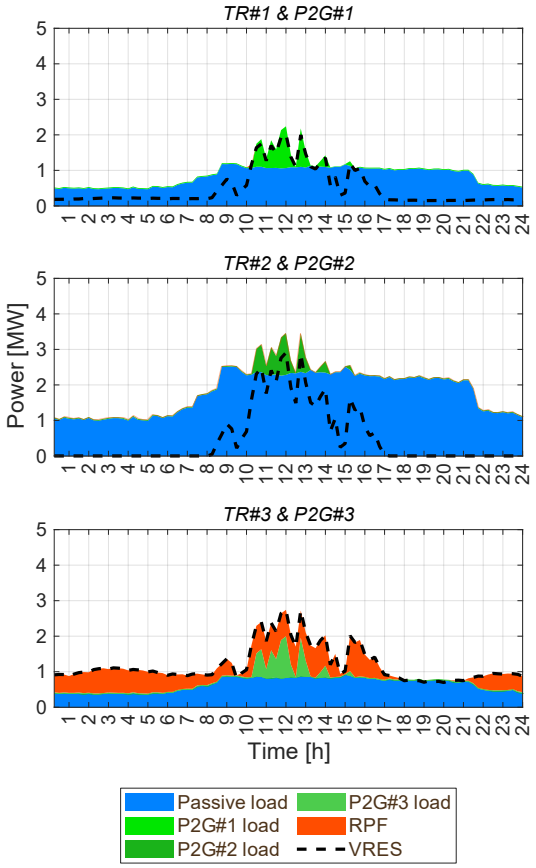

Figure 19. Electricity balance on HV/MV transformers (winter day) – LPEN simulation.

5.3. The value of gas network modeling

Unlike the reference model, the lumped parameter model does not take into account the pressure or gas flows in the gas network. Nevertheless, the results obtained with the lumped parameter model are almost the same as those of the Reference simulation, whenever only the heating season is considered (see Table A. 1-3). In these conditions, in fact, the production of SNG covers only 4% of the users' gas demand (see Table A. 3) and, at any time step, the production of SNG is considerably lower than the users' gas demand All the injected SNG is consumed directly by the users and this behavior is clearly simulated by both models (compare Figure 15 and Figure 20).

However, during the summer when the demand for gas is much lower, it is necessary to take into account the line-pack effect of the network in order to avoid underestimating the flexibility of the gas network. The LPGN model, not taking into account the gas flows and the pressure of the gas network, does not allow the line-pack of the network to be taken into account: SNG injection is limited in order to always be lower than the network gas demand (see Figure 21). Therefore, ignoring the intrinsic flexibility of the gas network limits the use of methane gas units, and, in the hot season, SNG production is underestimated by about 30% (see Table A. 3).

The limitation of the methanation units also affects the functioning of the electrolyzers: if the methanation units are unable to consume the hydrogen accumulated in the buffers, once the saturation of the hydrogen buffers is reached, the electrolyzers have to block their production of hydrogen, and, consequently, they are no longer able to offer flexibility to the electricity grid (see Figure 22). The underestimation of the flexibility of the gas network, induced as a result of the use of the simplified model, not only affects the gas network, but also the electricity network. In fact, the electrolyzers result to be less flexible and to cause an overestimation of almost 190% of the RPF generated by the HV/MV transformers during the hot season (see Table A. 2).

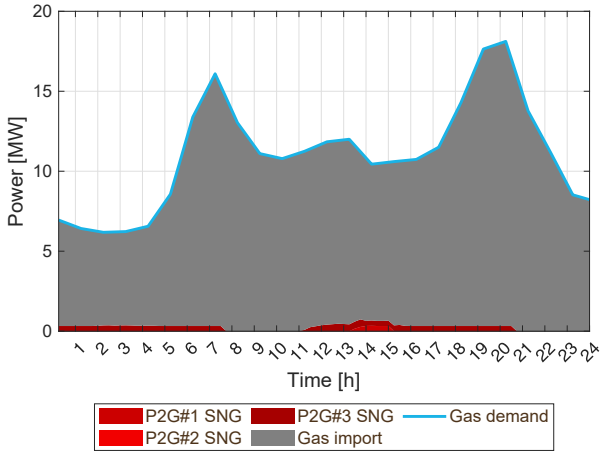

Figure 20. Gas network balance (winter day) – the LPGN simulation.

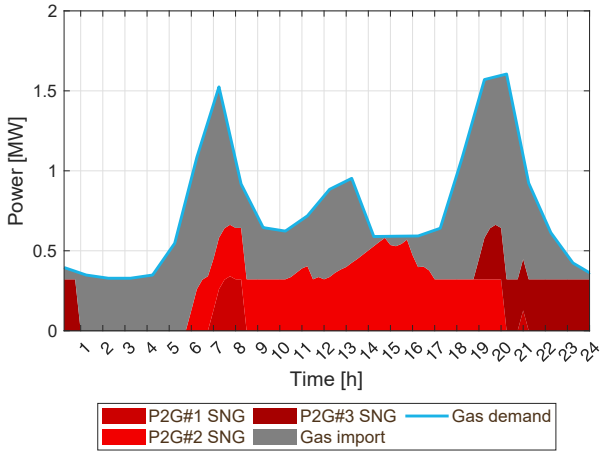

Figure 21. Gas network balance and pressure (summer day) – LPGN simulation.

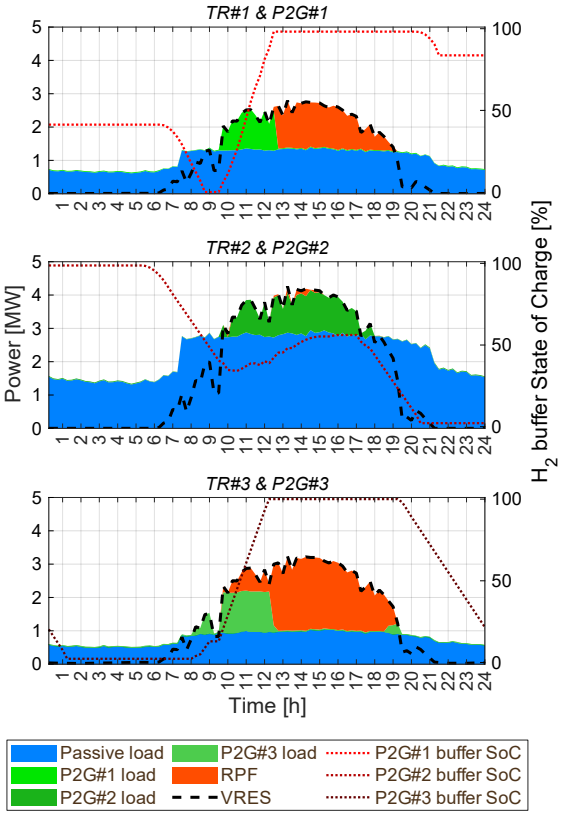

Figure 22. Electricity balance on HV/MV transformers and P2G hydrogen buffer SoC (summer day) – LPGN simulation.

5.4. The value of P2G modeling

The P2G lumped parameter model neglects the presence of the hydrogen buffer: in such an approach, the electricity energy is considered to be directly converted into SNG, without any possibility of storing hydrogen. Hence, the SNG production starts earlier than in the Reference simulation. Whenever the P2G reference model is used, the methanation units are only turned on when the hydrogen buffers have reached a predetermined state of charge (see Figure 23). It can be noted that the production of SNG in the LPP2G simulation case is less uniform than in the Reference simulation, as the lumped parameter model does not consider the ramp up and ramp down constraints of the plant, thus the SNG production follows the much faster variation characteristic of the electrolyzers. Apart from this misalignment, the use of this simplification during the heating season, when there is a high gas demand, does not change the simulation results to any great extent (see Table A. 1-3). The small differences that can be seen in Table A. 1, which are lower than 4 %, are mainly due to the fact that the reference model takes into account the change in energy conversion efficiency for different working conditions, while the lumped parameter model considers a constant average efficiency.

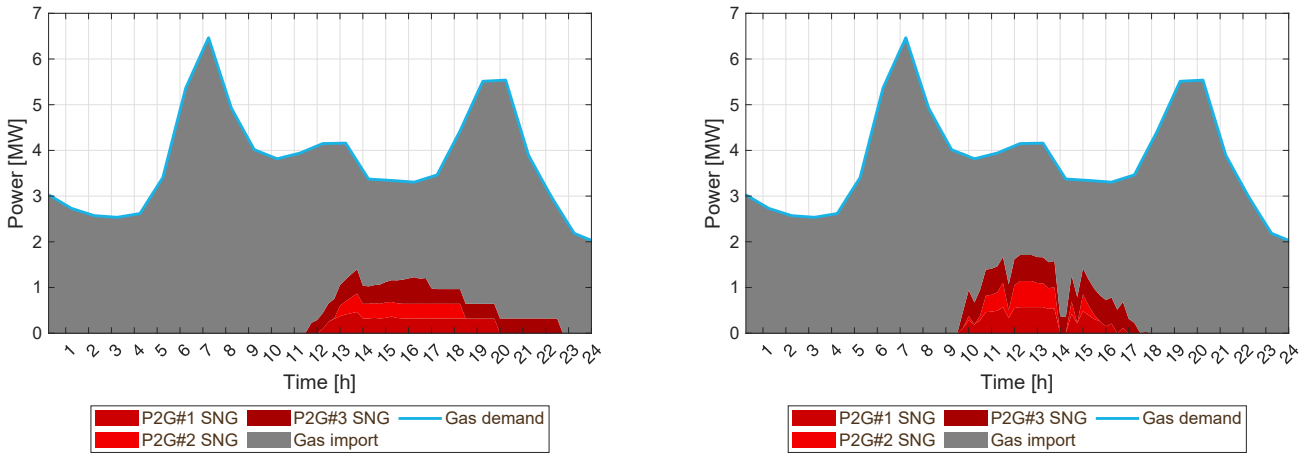

Figure 23. Gas network balance (mid-season day) – (a) Reference simulation and (b) LPP2G simulation.

However, in the summer season, due to the low gas demand, the gas network becomes less flexible, as it can accept a smaller quantity of SNG. In this case, neglecting the flexibility given by the decoupling of the methanation units from the electrolyzers affects the results of the simulation. In fact, when the gas network reaches the maximum allowed pressure, the electrolyzers can continue to work by accumulating the hydrogen produced inside the buffer. On the other hand, in the case of LPP2G, when the pressure in the gas network reaches its maximum limit at 12:45 (see Figure 24), the electrolyzers also have to limit their loads (see Figure 25).

It should be noted that, even in the Reference simulation, the electrolyzer may be affected by restrictions (see P2G#1 in Figure 16): this may happen when the hydrogen buffer reaches it maximum SoC, and the hydrogen production needs to be reduced to prevent an overpressure being created in the buffer. Nevertheless, without considering the hydrogen buffer, the P2G plants have less flexibility, which leads to the P2G potential being underestimated during the low gas demand period (i.e., in the summer season), and the use of P2G plants being underestimated by about 10%, which is also reflected by an equal underestimation of the SNG injection in the gas network. Moreover, the RPF on the electricity network is overestimated by about 150 % (see Table A. 1-3).

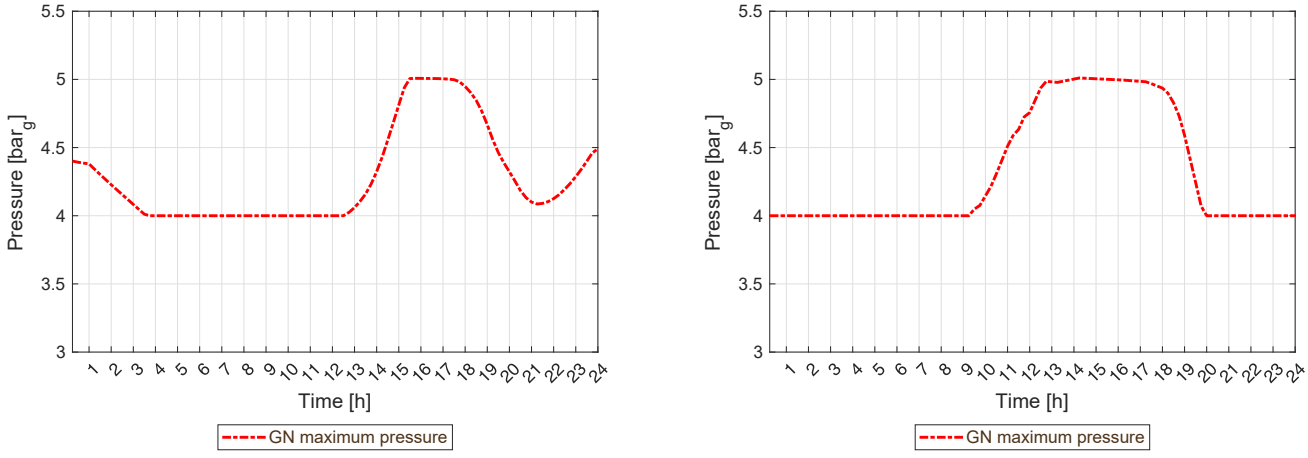

Figure 24. Gas network pressure (summer day) – (a) Reference simulation and (b) LPP2G simulation.

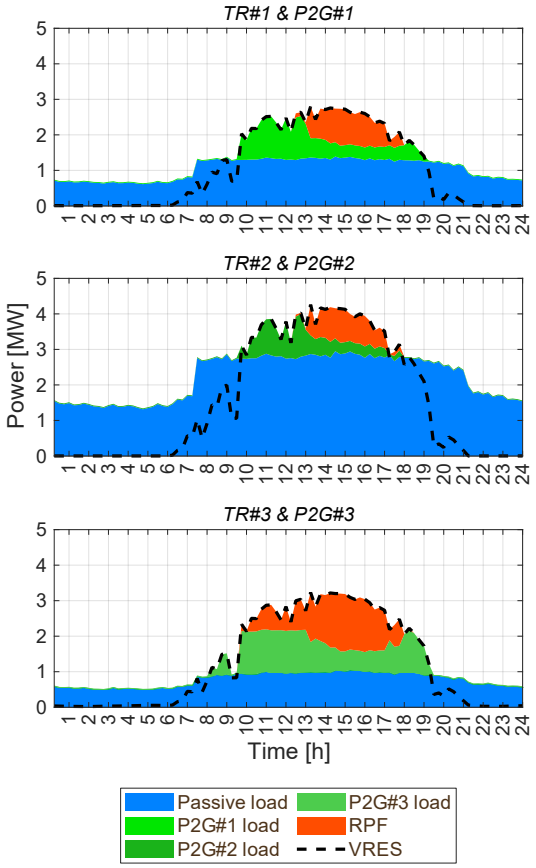

Figure 25. Electricity balance on HV/MV transformers (summer day) – LPP2G simulation.

6. Conclusions

This article discusses the use of P2G technology to balance VRES production at the distribution level. On the one hand, the P2G plants, thanks to their flexibility, were able to absorb the local over-generations of VRES that can cause an RPF at the electricity distribution level. On the other hand, with a high gas demand (e.g., in a typical winter case in which gas is used for heating), P2G systems can operate without any production constraints. However, when this technology is connected to the gas distribution network, restrictions may occur in its operation in low gas demand periods. Nonetheless, the flexibility offered by the line-pack effect within the gas network and the flexibility enabled by the hydrogen buffers, allow P2G to be used, even in these conditions.

The study presents a methodological analysis of the impact of different simulation approaches for multi-energy system operation scenarios. Critical conditions can easily arise for the operation of P2G at the distribution level; hence, the choice of the most appropriate modeling approaches is necessary in order to correctly simulate the dynamics between the various components of the multi-energy system (the electricity network, the gas network and P2G plants) and to avoid the overestimation or underestimate of the flexibility potential.

The results obtained using detailed models of the three components have been compared with those obtained from simulating scenarios in which different modeling aspects had been neglected. Different simulations were carried out, in which the following aspects were neglected one at a time: (*i*) the topology of the electricity distribution network and, consequently, the local power flows that occur within it, (*ii*) the topology of the gas network, the gas flows and the evolution of the network pressure and (*iii*) the intermediate energy conversion processes and storage that can occur in P2G plants between electricity and SNG.

The main conclusions that can be drawn from these analyses can be summarized as follows:

i. *Distribution System Modeling*: taking into account the topology of the electricity network makes it possible to evaluate in which area of the electricity network the over-generations of renewable energy occur and therefore allows one to choose the most appropriate resources to use, i.e., those closest to the electricity unbalances. Thus, the use of an electricity network model allows both the dispatching of flexible resources to be optimized and the best connection nodes for these resources to be evaluated.

- It is essential to consider electricity distribution network power flows if flexible resources are used to optimize the distribution network. Local VRES over-generations can only be highlighted by taking into account the distribution network topology. It is useful to analyze these phenomena as they can create RPFs on HV/MV transformers, thus leading to problems concerning the operation of the distribution system. The local over-generations of renewables can be mitigated, thanks to distributed flexible resources: thus, if these local imbalances are not detected, the potential benefit of using flexible distributed resources is underestimated.

- The single node representation of the electricity system cannot detect local overproductions. Nevertheless, it may be employed to evaluate whether it would be useful to offer the flexibility resources to TSO services for the operation of the transmission system.

ii. *Gas Grid Modeling*: simulating the dynamics of the gas network makes it possible to have a more precise evaluation of the flexibility offered by this infrastructure, because the gas network can be used to store the production of SNG, thanks to the line-pack effect. This storage is possible as long as the pressure in the network remains within the allowable pressure range. Hence, the gas network acts like a gas storage device, by allowing the gas demand to be decoupled from the SNG production.

- The gas network flexibility may be relatively low in low gas demand periods: under certain conditions, the gas withdrawal can be lower than the SNG injection. When this happens, the gas network can reach saturation; thus, the SNG injections should be limited. Under these conditions, it is possible to evaluate the line-pack potential and, hence, the flexibility of the gas network by considering the gas flows and the network pressure evolution. Since all the components in a multi-energy system scenario are closely connected, an underestimation of the gas network flexibility implies a lower flexibility of the connected P2G plants, which in turn leads to an underestimation of their utilization and also affects the operation of the electricity network (measured as a residual RPF).
- The gas demand in a high gas demand scenario is normally much higher than for SNG injections. Such a high gas withdrawal improves the flexibility of the gas network, because the injected SNG may be absorbed directly by the users, without causing network saturation problems. In this case, the line-pack flexibility of the network may be neglected, without affecting the simulation results.

iii. *P2G Plant Modeling*: a physical model of a P2G plant allows all the processes that take place in a P2G plant to be simulated. This permits a decoupling between the methanation unit and the electrolyzer to be considered. The electrolyzer can therefore work even when, due to external restrictions, the methanation unit cannot operate. Taking these factors into account allows the flexibility of these plants to be properly estimated.

- On the one hand, in low gas demand periods, when the flexibility of the gas network is lower, the utilization of P2G plants may be constrained, because no SNG injection is allowed. In these circumstances, neglecting the interactions between the various components of the P2G system leads to an underestimation of the P2G flexibility, and, therefore, an underestimation of both the possible SNG production and the services that these resources can offer to the electricity system.
- On the other hand, in high gas demand periods, the flexibility offered by the gas network is high enough to compensate for the underestimation of the flexibility of the P2G plant. In these conditions, the utilization of a simplified model that does not simulate the entire electricity-hydrogen-SNG chain allows the energy flows within the multi-energy system to be evaluated at a good level of approximation.

Future works will focus on using these modeling hints to evaluate the possibility of locally managing multi-energy systems, that is, implementing the concept of multi-energy microgrids. In such a case, the electricity network dynamics will take on a more important role, as will the consequent stress that the flexibility components have to sustain. Furthermore, new infrastructures, such as district heating and building storage, will be integrated by delineating a complete technical evaluation of the calculation tools that should be used for the design of future urban areas within the "smart cities paradigm".

Appendix A. Simulation data results

Table A. 1. P2G plant results.

	Unit	Heating season				Non-heating season				Whole year			
		P2G#1	P2G#2	P2G#3	Tot	P2G#1	P2G#2	P2G#3	Tot	P2G#1	P2G#2	P2G#3	Tot
Reference simulation													
El. cons	GWh	0.72	0.50	1.69	2.90	1.32	0.98	2.14	4.44	2.03	1.48	3.83	7.34
SNG	GWh	0.29	0.19	0.79	1.27	0.58	0.40	1.02	2.01	0.87	0.59	1.81	3.27
Lumped parameter electricity network (LPEN) simulation													
El. cons	GWh	0.80	0.80	0.80	2.40	1.44	1.43	1.40	4.26	2.23	2.23	2.20	6.66
SNG	GWh	0.33	0.33	0.33	1.00	0.64	0.64	0.62	1.91	0.98	0.97	0.96	2.90
Lumped parameter gas network (LPGN) simulation													
El. cons	GWh	0.71	0.50	1.68	2.90	0.85	0.81	1.56	3.23	1.57	1.31	3.25	6.12
SNG	GWh	0.29	0.19	0.79	1.27	0.35	0.34	0.72	1.42	0.64	0.53	1.51	2.68
Lumped parameter P2G (LPP2G) simulation													
El. cons	GWh	0.72	0.50	1.70	2.92	1.04	0.76	1.97	3.77	1.76	1.26	3.67	6.69
SNG	GWh	0.30	0.19	0.78	1.27	0.46	0.32	0.91	1.69	0.76	0.52	1.69	2.96

Table A. 2. Electricity network results.

	Unit	Heating season				Non-heating season				Whole year			
		TR#1	TR#2	TR#3	Tot	TR#1	TR#2	TR#3	Tot	TR#1	TR#2	TR#3	Tot

Reference simulation													
EL demand	GWh	3.70	7.80	2.79	14.29	4.12	8.71	2.97	15.80	7.82	16.50	5.76	30.08
VRES	GWh	2.41	3.23	4.12	9.76	3.90	5.68	5.39	14.97	6.32	8.91	9.51	24.73
Surplus	GWh	0.67	0.46	2.04	3.17	1.40	1.08	3.08	5.55	2.07	1.54	5.11	8.72
Absorbed surplus	GWh	0.62	0.40	1.61	2.63	1.23	0.90	2.07	4.20	1.86	1.30	3.68	6.83
RPF	GWh	0.05	0.06	0.43	0.53	0.16	0.18	1.01	1.35	0.21	0.24	1.44	1.88
Lumped parameter electricity network (LPEN) simulation													
EL demand	GWh	-	-	-	14.29	-	-	-	15.80	-	-	-	30.08
VRES	GWh	-	-	-	9.76	-	-	-	14.97	-	-	-	24.73
Surplus	GWh	-	-	-	2.45	-	-	-	5.09	-	-	-	7.54
Absorbed surplus	GWh	-	-	-	1.98	-	-	-	3.80	-	-	-	5.78
RPF	GWh	-	-	-	0.46	-	-	-	1.29	-	-	-	1.76
Lumped parameter gas network (LPGN) simulation													
EL demand	GWh	3.70	7.80	2.79	14.29	4.12	8.71	2.97	15.80	7.82	16.50	5.76	30.08
VRES	GWh	2.41	3.23	4.12	9.76	3.90	5.68	5.39	14.97	6.32	8.91	9.51	24.73
Surplus	GWh	0.67	0.46	2.04	3.17	1.40	1.08	3.08	5.55	2.07	1.54	5.11	8.72
Absorbed surplus	GWh	0.62	0.40	1.61	2.63	0.77	0.73	1.49	2.98	1.39	1.13	3.10	5.61
RPF	GWh	0.05	0.06	0.43	0.54	0.63	0.35	1.59	2.57	0.68	0.41	2.02	3.10
Lumped parameter P2G (LPP2G) simulation													
EL demand	GWh	3.65	7.74	2.74	14.13	4.07	8.66	2.91	15.64	7.72	16.40	5.65	29.77
VRES	GWh	2.41	3.23	4.12	9.76	3.90	5.68	5.39	14.97	6.32	8.91	9.51	24.73
Surplus	GWh	0.68	0.47	2.06	3.21	1.42	1.09	3.10	5.61	2.10	1.56	5.17	8.82
Absorbed surplus	GWh	0.64	0.41	1.65	2.70	0.98	0.68	1.92	3.58	1.61	1.10	3.57	6.28
RPF	GWh	0.04	0.06	0.42	0.51	0.44	0.41	1.18	2.03	0.48	0.46	1.60	2.55

Table A. 3. Gas network results.

	Unit	Heating season	Non-heat. season	Whole year
Reference simulation				
Gas demand	GWh	31.65	4.37	36.02
Imported Gas	GWh	30.38	2.37	32.75
Imported Gas	GWh	1.27	2.00	3.27
Lumped parameter electricity network (LPEN) simulation				
Gas demand	GWh	31.65	4.37	36.02
Imported Gas	GWh	30.65	2.47	33.12
SNG	GWh	1.00	1.91	2.90
Lumped parameter gas network (LPGN) simulation				
Gas demand	GWh	31.65	4.37	36.02
Imported Gas	GWh	30.38	2.96	33.34
SNG	GWh	1.27	1.42	2.68
Lumped parameter P2G (LPP2G) simulation				
Gas demand	GWh	31.65	4.37	36.02
Imported Gas	GWh	30.38	2.68	33.06
SNG	GWh	1.27	1.69	2.96

References

[1] Rogelj J, Luderer G, Pietzcker RC, Kriegler E, Schaeffer M, Krey V, Riahi K. Energy system transformations for limiting end-of-century warming to below 1.5 °C. Nature Climate Change. 2015;5:519–27. https://doi.org/10.1038/nclimate2572.

[2] European Commission. Clean energy for all Europeans. Luxembourg (Belgium) 2019. https://doi.org/10.2833/9937.

[3] Bertsch J, Growitsch C, Lorenczik S, Nagl S. Flexibility in Europe's power sector-An additional requirement or an automatic complement? Energy Economics. 2016;53:118–31. https://doi.org/10.1016/j.eneco.2014.10.022.

[4] Impram S, Nese SV, Oral B. Challenges of renewable energy penetration on power system flexibility: A survey. Energy Strategy Reviews. 2020;31:100539. https://doi.org/10.1016/j.esr.2020.100539.

[5] Babatunde OM, Munda JL, Hamam Y. Power system flexibility: A review. Energy Reports. 2020;6:101-6. https://doi.org/10.1016/j.egyr.2019.11.048.

[6] Badami M, Fambri G, Mancò S, Martino M, Damousis IG, Agtzidis D, Tzovaras D. A decision support system tool to manage the flexibility in renewable energy-based power systems. Energies. 2020;13(1):153. https://doi.org/10.3390/en13010153.

[7] Li N, Uckun C, Constantinescu EM, Birge JR, Hedman KW, Botterud A. Flexible Operation of Batteries in Power System Scheduling with Renewable Energy. IEEE Transactions on Sustainable Energy. 2016;7:685–96. https://doi.org/10.1109/TSTE.2015.2497470.

[8] Simão M, Ramos HM. Hybrid pumped hydro storage energy solutions towards wind and PV integration: Improvement on flexibility, reliability and energy costs. Water. 2020;12. https://doi.org/10.3390/w12092457.

[9] Amoli NA, Meliopoulos APS. Operational flexibility enhancement in power systems with high penetration of wind power using compressed air energy storage. In 2015 Clemson University power systems conference (PSC). 2015, Clemson, SC, USA: IEEE; 2015. https://doi.org/10.1109/PSC.2015.7101694.

[10] Lund H, Østergaard PA, Connolly D, Ridjan I, Mathiesen BV, Hvelplund F, et al. Energy storage and smart energy systems. International Journal of Sustainable Energy Planning and Management. 2016;11:3–14. https://doi.org/10.5278/ijsepm.2016.11.2.

[11] Chicco G, Riaz S, Mazza A, Mancarella P. Flexibility from Distributed Multienergy Systems. Proceedings of the IEEE. 2020;108:1496–517. https://doi.org/10.1109/JPROC.2020.2986378.

[12] Mathiesen B V, Lund H, Connolly D, Wenzel H, Ostergaard PA, Möller B, et al. Smart Energy Systems for coherent 100% renewable energy and transport solutions. Applied Energy. 2015;145:139–54. https://doi.org/10.1016/j.apenergy.2015.01.075.

[13] Fambri G, Badami M, Tsagkrasoulis D, Katsiki V, Giannakis G, Papanikolaou A. Demand flexibility enabled by virtual energy storage to improve renewable energy penetration. Energies. 2020;13(19):5128. https://www.mdpi.com/1996-1073/13/19/5128.

[14] Troitzsch S, Sreepathi BK, Huynh TP, Moine A, Hanif S, Fonseca J, Hamacher T. Optimal electric-distribution-grid planning considering the demand-side flexibility of thermal building systems for a test case in Singapore. Applied Energy. 2020;273:114917. https://doi.org/10.1016/j.apenergy.2020.114917.

[15] Diaz-Londono C, Colangelo L, Ruiz F, Patino D, Novara C, Chicco G. Optimal strategy to exploit the flexibility of an electric vehicle charging station. Energies. 2019;12(20):3834. https://doi.org/10.3390/en12203834.

[16] Schuller A, Flath CM, Gottwalt S. Quantifying load flexibility of electric vehicles for renewable energy integration. Applied Energy. 2015;151:335-44. http://dx.doi.org/10.1016/j.apenergy.2015.04.004.

[17] Østergaard PA, Andersen AN. Variable taxes promoting district heating heat pump flexibility. Energy. 2021;15;221:119839. https://doi.org/10.1016/j.energy.2021.119839.

[18] Coccia G, Mugnini A, Polonara F, Arteconi A. Artificial-neural-network-based model predictive control to exploit energy flexibility in multi-energy systems comprising district cooling. Energy. 2021;222:119958. https://doi.org/10.1016/j.energy.2021.119958.

[19] Zhang F, Salimu A, Ding L. Operation and optimal sizing of combined P2G-GfG unit with gas storage for frequency regulation considering curtailed wind power. International Journal of Electrical Power & Energy Systems. 2022;141:108278. https://doi.org/10.1016/j.ijepes.2022.108278.

[20] Mansouri SA, Nematbakhsh E, Ahmarinejad A, Jordehi AR, Javadi MS, Matin SA. A multi-objective dynamic framework for design of energy hub by considering energy storage system, power-to-gas technology and integrated demand response program. Journal of Energy Storage. 2022;50:104206. https://doi.org/10.1016/j.est.2022.104206.

[21] Mansouri SA, Ahmarinejad A, Nematbakhsh E, Javadi MS, Jordehi AR, Catalão JP. Energy hub design in the presence of P2G system considering the variable efficiencies of gas-fired converters. In2021 International Conference on Smart Energy Systems and Technologies (SEST). IEEE. 2021;1-6. https://doi.org/10.1109/SEST50973.2021.9543179.

[22] Nasir M, Jordehi AR, Matin SA, Tabar VS, Tostado-Véliz M, Mansouri SA. Optimal operation of energy hubs including parking lots for hydrogen vehicles and responsive demands. Journal of Energy Storage. 2022;50:104630. https://doi.org/10.1016/j.est.2022.104630.

[23] MansourLakouraj M, Shams MH, Niaz H, Liu JJ, Javadi MS, Catalão JP. Optimal Coordination of Hydrogen Vehicle Stations and Flexible Resources in Microgrids. In2021 IEEE International Conference on Environment and Electrical Engineering and 2021 IEEE Industrial and Commercial Power Systems Europe (EEEIC/I&CPS Europe). IEEE. 2021;1-6. https://doi.org/10.1109/EEEIC/ICPSEurope51590.2021.9584761.

[24] Barelli L, Bidini G, Ottaviano PA, Perla M. Liquefied Synthetic Natural Gas Produced through Renewable Energy Surplus: Impact Analysis on Vehicular Transportation by 2040 in Italy. Gases. 2021;1(2):80-91. https://doi.org/10.3390/gases1020007.

[25] Glenk G, Reichelstein S. Reversible Power-to-Gas systems for energy conversion and storage. Nature communications. 2022;13(1):1-0. https://doi.org/10.1038/s41467-022-29520-0.

[26] Shams MH, MansourLakouraj M, Liu JJ, Javadi MS, Catalão JP. Bi-level Two-stage Stochastic Operation of Hydrogen-based Microgrids in a Distribution System. In2021 International Conference on Smart Energy Systems and Technologies (SEST). IEEE. 2021;1-6. https://doi.org/10.1109/SEST50973.2021.9543410.

[27] Kötter E, Schneider L, Sehnke F, Ohnmeiss K, Schröer R. The future electric power system: Impact of Power-to-Gas by interacting with other renewable energy components. Journal of Energy Storage. 2016;5:113–9. https://doi.org/10.1016/j.est.2015.11.012.

[28] Weiss R, Savolainen J, Peltoniemi P, Inkeri E. Optimal scheduling of a P2G plant in dynamic power, heat and gas markets. In10th International Renewable Energy Storage (IRES 2016). EUROSOLAR. 2016, Düsseldorf, Germany.

[29] Weiss R, Kannari L, Pennanen J, Sihvonen T, Savolainen J. Optimal Co-Production of Market Based Power Grid Support and Renewable Fuels or Chemicals. In 2016 AIChE Annual Meeting: Sustainable Engineering Forum 2016. American Institute of Chemical Engineers (AIChE). 2016;250-257.

[30] Blanco H, Nijs W, Ruf J, Faaij A. Potential of Power-to-Methane in the EU energy transition to a low carbon system using cost optimization. Applied Energy. 2018;232:323–40. https://doi.org/10.1016/j.apenergy.2018.08.027.
[31] Belderbos A, Valkaert T, Bruninx K, Delarue E, D'haeseleer W. Facilitating renewables and power-to-gas via integrated electrical power-gas system scheduling. Applied Energy. 2020;275:115082. https://doi.org/10.1016/j.apenergy.2020.115082.
[32] Xi Y, Fang J, Chen Z, Zeng Q, Lund H. Optimal coordination of flexible resources in the gas-heat-electricity integrated energy system. Energy. 2021;223:119729. https://doi.org/10.1016/j.energy.2020.119729.
[33] Ikäheimo J, Weiss R, Kiviluoma J, Pursiheimo E, Lindroos TJ. Impact of power-to-gas on the cost and design of the future low-carbon urban energy system. Applied Energy. 2022; 305: 117713. https://doi.org/10.1016/j.apenergy.2021.117713.
[34] Mazza A, Salomone F, Arrigo F, Bensaid S, Bompard E, Chicco G. Impact of Power-to-Gas on distribution systems with large renewable energy penetration. Energy Conversion and Management: X. 2020;7:100053. https://doi.org/10.1016/j.ecmx.2020.100053.
[35] Robinius M, Raje T, Nykamp S, Rott T, Müller M, Grube T, et al. Power-to-Gas: Electrolyzers as an alternative to network expansion – An example from a distribution system operator. Applied Energy. 2018;210:182–97. https://doi.org/10.1016/j.apenergy.2017.10.117.
[36] El-Taweel NA, Khani H, Farag HEZ. Voltage regulation in active power distribution systems integrated with natural gas grids using distributed electric and gas energy resources. International Journal of Electrical Power & Energy Systems. 2019;106:561–71. https://doi.org/10.1016/j.ijepes.2018.10.037.
[37] Council of the European Union EP. Regulation (EU) 2019/943 of the European Parliament and of the Council of 5 June 2019 on the internal market for electricity. vol. 62. 2019.
[38] The SmartNet Consortium. TSO-DSO Coordination for Acquiring Ancillary Services From Distribution Grids. 2019.
[39] Estermann T, Newborough M, Sterner M. Power-to-gas systems for absorbing excess solar power in electricity distribution networks. International Journal of Hydrogen Energy. 2016;41:13950–9. https://doi.org/10.1016/j.ijhydene.2016.05.278.
[40] Dalmau AR, Perez DM, Diaz De Cerio Mendaza I, Pillai JR. Decentralized voltage control coordination of on-load tap changer transformers, distributed generation units and flexible loads. In 2015 IEEE Innovative Smart Grid Technologies-Asia (ISGT ASIA). IEEE. 2015. https://doi.org/10.1109/ISGT-Asia.2015.7386966.
[41] Diaz De Cerio Mendaza I, Bhattarai BP, Kouzelis K, Pillai JR, Bak-Jensen B, Jensen A. Optimal sizing and placement of power-to-gas systems in future active distribution networks. . In 2015 IEEE Innovative Smart Grid Technologies-Asia (ISGT ASIA). IEEE. 2015. https://doi.org/10.1109/ISGT-Asia.2015.7387053.
[42] Mazza A, Cavana M, Medina EL, Chicco G, Leone P. Creation of representative gas distribution networks for multi-vector energy system studies. In 2019 IEEE International Conference on Environment and Electrical Engineering and 2019 IEEE Industrial and Commercial Power Systems Europe (EEEIC/I&CPS Europe). IEEE. 2019;1-6. https://doi.org/10.1109/EEEIC.2019.8783701.
[43] Cavana M, Mazza A, Chicco G, Leone P. Electrical and gas networks coupling through hydrogen blending under increasing distributed photovoltaic generation. Applied Energy. 2021;290:116764. https://doi.org/10.1016/j.apenergy.2021.116764.
[44] Diaz-Londono C, Fambri G, Mazza A, Badami M, Bompard E. A Real-Time Based Platform for Integrating Power-to-Gas in Electrical Distribution Grids. In 2020 55th International Universities Power Engineering Conference (UPEC 2020). IEEE. 2020;1–6. https://doi.org/10.1109/UPEC49904.2020.9209803.
[45] Weiss R, Saastamoinen H, Ikäheimo J, Abdurafikov R, Sihvonen T, Shemeikka J. Decarbonised district heat, electricity and synthetic renewable gas in wind-and solar-based district energy systems. Journal of Sustainable Development of Energy, Water and Environment Systems. 2021;9(2):1-22. https://doi.org/10.13044/j.sdewes.d8.0340.
[46] Salomone F, Giglio E, Ferrero D, Santarelli M, Pirone R, Bensaid S. Techno-economic modelling of a Power-to-Gas system based on SOEC electrolysis and CO2 methanation in a RES-based electric grid. Chemical Engineering Journal. 2019;377:120233. https://doi.org/10.1016/j.cej.2018.10.170.
[47] Khani H, El-Taweel N, Farag HEZ. Real-time optimal management of reverse power flow in integrated power and gas distribution grids under large renewable power penetration. IET Generation, Transmission & Distribution. 2018;12:2325–31. https://doi.org/10.1049/iet-gtd.2017.1513.
[48] Fambri G, Diaz-Londono C, Mazza A, Badami M, Weiss R. Techno-economic analysis of Power-to-Gas plants in a gas and electricity distribution network system with high renewable energy penetration. Applied Energy. 2022;312:118743. https://doi.org/10.1016/j.apenergy.2022.118743.
[49] Badami M, Fambri G. Optimising energy flows and synergies between energy networks. Energy. 2019;173:400–12. https://doi.org/10.1016/j.energy.2019.02.007.
[50] Clegg S, Mancarella P. Integrated modeling and assessment of the operational impact of power-to-gas (P2G) on electrical and gas transmission networks. IEEE Transactions on Sustainable Energy. 2015;6(4):1234-44. https://doi.org/10.1109/TSTE.2015.2424885.
[51] Clegg S, Mancarella P. Storing renewables in the gas network: modelling of power-to-gas seasonal storage flexibility in low-carbon power systems. IET Generation, Transmission & Distribution. 2016;10(3):566-75. https://doi.org/10.1049/iet-gtd.2015.0439.
[52] Badami M, Bompard E, Diaz-Londono C, Fambri G, Mazza A, Verda V. Deliverable D3.6 PLANET simulation model generator and integration to the distribution grid simulation suite. PLANET 2020. Available online: https://www.h2020-

planet.eu/deliverables.
[53] Cavana M, Leone P. Biogas blending into the gas grid of a small municipality for the decarbonization of the heating sector. Biomass and Bioenergy. 2019;127:105295. https://doi.org/10.1016/j.biombioe.2019.105295.
[54] Italian Ministry of the Interior. Norme di sicurezza antincendio per il trasporto, la distribuzione, l'accumulo e l'utilizzazione del gas naturale con densità non superiore a 0,8 (report in Italian). 1984;40. Available online: https://www.certifico.com/component/attachments/download/12396.
[55] Kersting WH. Distribution System Modeling and Analysis. CRC press. Boca Raton, CA, USA, 2017. https://doi.org/10.1201/9781315120782.
[56] Barrero-González F, Pires VF, Sousa JL, Martins JF, Milanés-Montero MI, González-Romera E, Romero-Cadaval E. Photovoltaic Power Converter Management in Unbalanced Low Voltage Networks with Ancillary Services Support. Energies. 2019;12;972. https://doi.org/10.3390/en12060972.
[57] Shirmohammadi D, Hong HW, Semlyen A, Luo GX. A compensation-based power flow method for weakly meshed distribution and transmissionnetworks. IEEE Transactions on power systems. 1988;3(2):753-62. https://doi.org/10.1109/59.192932.
[58] Horn RA, Johnson CR. Matrix analysis. Cambridge university press; 2012. https://doi.org/10.1017/CBO9780511810817.
[59] SNAM. Codice di rete SNAM rete gas. 2012;486 (report in Italian). Available online: https://www.snam.it/export/sites/snam-rp/repository-srg/file/Codice_di_rete/05_Archivio_CdR/2012/33.Codice_di_Rete_RevXXXIII.pdf.
[60] Fischer D, Kaufmann F, Selinger-Lutz O, Voglstätter C. Power-to-gas in a smart city context–Influence of network restrictions and possible solutions using on-site storage and model predictive controls. International Journal of Hydrogen Energy. 2018;43(20):9483-94. https://doi.org/10.1016/j.ijhydene.2018.04.034.
[61] Savolainen J, Kannari L, Pennanen J, Tähtinen M, Sihvonen T, Pasonen R, Weiss R. Operation of a PtG plant under power scheduling. 10th Int. Renew. Energy Storage. Conf. IRES 2016, Düsseldorf, Germany: EUROSOLAR; 2016.
[62] Eero S, Kaj J, Markku H, Olli T, Jorma K, Kari P. The APROS software for process simulation and model development. VTT Technical Research Centre of Finland; 1989.
[63] Wilson ZT, Sahinidis NV. The ALAMO approach to machine learning. Computers & Chemical Engineering. 2017 Nov 2;106:785-95. https://doi.org/10.1016/j.compchemeng.2017.02.010.
[64] Badami M, Verda V, Mazza A, Fambri G, Weiss R, Savolainen J, et al. Deliverable D2.5 Power-to-Gas process / system models. PLANET 2020. Available online: https://www.h2020-planet.eu/deliverables.
[65] Savolainen J, Kannari L, Pennanen J, Tähtinen M, Sihvonen T, Pasonen R, Weiss R. Operation of a PtG plant under power scheduling. In 10th International Renewable Energy Storage. IRES 2016. Düsseldorf, Germany, 2016.
[66] Marocco P, Ferrero D, Lanzini A, Santarelli M. Optimal design of stand-alone solutions based on RES+ hydrogen storage feeding off-grid communities. Energy Conversion and Management. 2021;238:114147. https://doi.org/10.1016/j.enconman.2021.114147.
[67] TRACTEBEL ENGINEERING S.A. and Hinicio. Study on Early Business Cases for H2 in Energy Storage and More Broadly Power To H2 Applications. 2017;228. Available online https://www.fch.europa.eu/sites/default/files/P2H_Full_Study_FCHJU.pdf.